Zanthoxylum zanthoxyloides inhibits lipopolysaccharide- and synthetic hemozoin-induced neuroinflammation in BV-2 microglia: roles of NF-κB transcription factor and NLRP3 inflammasome activation

Folashade A Ogunrinade[a], Stephanie T Guetchueng[b,e], Folashade O Katola[a], Mutalib A Aderogba[c], Idowu S. Akande[d], Satyajit D Sarker[b], Olumayokun A Olajide[a*]

[a] Department of Pharmacy, School of Applied Sciences, University of Huddersfield, Huddersfield, HD1 3DH, United Kingdom

[b] Centre for Natural Products Discovery, School of Pharmacy and Biomolecular Sciences, Liverpool John Moores University, Byrom Street, Liverpool L3 3AF, United Kingdom

[c] Department of Chemistry, Faculty of Science, Obafemi Awolowo University, Ile-Ife, Nigeria

[d] Department of Biochemistry, College of Medicine, University of Lagos, Nigeria

[e] Current Address: Institute of Medical Research and Medicinal Plants Studies, Yaounde, Cameroon

***Author for Correspondence**

Dr Olumayokun Olajide

Department of Pharmacy, School of Applied Sciences

University of Huddersfield

Queensgate

Huddersfield, HD1 3DH

United Kingdom

Email: o.a.olajide@hud.ac.uk

Telephone: +44 (0) 1484 472735

Abstract

Objectives: The effects of a root extract of *Zanthoxylum zanthoxyloides* on neuroinflammation in BV-2 microglia stimulated with LPS and hemozoin were investigated.

Methods: ELISA, enzyme immunoassay and Griess assay were used to evaluate levels of cytokines, PGE_2 and NO in culture supernatants, respectively. Microglia-mediated neurotoxicity was evaluated using a BV-2 microglia-HT-22 neuron transwell co-culture.

Key findings: Treatment with *Z. zanthoxyloides* caused reduced elevated levels of TNFα, IL-6, IL-1β, NO, and PGE_2, while increasing the levels of IL-10. In addition, there were reduced levels of iNOS and COX-2 proteins. This was accompanied by a prevention of microglia-mediated damage to HT-22 mouse hippocampal neurons. *Z. zanthoxyloides* reduced elevated levels phospho-IκB and of phospho-p65, while preventing degradation of IκB protein and DNA binding of p65. Further mechanistic studies revealed that *Z. zanthoxyloides* reduced the levels of pro-IL-1β and IL-1β in hemozoin-activated BV-2 microglia. This was accompanied by a reduction in caspase-1 activity and NLRP3 protein expression. Bioassay-guided fractionation resulted in the isolation of skimmianine as an anti-inflammatory compound in *Z. zanthoxyloides*.

Conclusion: This is the first report showing inhibition of neuroinflammation in LPS- and hemozoin-activated BV-2 microglia by the root extract of *Z. zanthoxyloides* by targeting the activation of both NF-κB and NLRP3 inflammasome.

Keywords: *Zanthoxylum zanthoxyloides*; Microglia, Lipopolysaccharide; Hemozoin; NLRP3; NF-κB

Introduction

Chronic neuroinflammation remains a critical component of the pathological mechanisms involved in neurodegenerative disorders such as Alzheimer's disease (AD), Parkinson's disease (PD), among others [1]. In particular, microglia-mediated neuroinflammation and excessive production of neurotoxic mediators have been strongly linked to the pathogenesis of AD [2,3]. In addition to direct neurotoxic effects, activated microglia also promote amyloid deposition during neuroinflammation [4]. With regards to PD, emerging evidence continues to link the pathogenesis of the disorder with neuroinflammation [5]. In PD, pro-inflammatory cytokines, chemokines, and other inflammatory proteins trigger microglial activation, which damage the nigrostriatal pathway [6]. These and other reports of advances in the understanding of the role played by microglia-mediated chronic neuroinflammation in neurodegenerative diseases suggest that it is a potential target for drugs.

Neuroinflammation has also been linked to the pathogenesis of cerebral malaria (CM), a parasitic infection caused by *Plasmodium falciparum*. This connection is evidenced by several animal and human studies which reported a correlation between serum concentrations of pro-inflammatory cytokines and chemokines and the severity of CM [7,8]. The role of neuroinflammation in CM was confirmed by studies reporting that the neurocognitive deficits in the condition is linked to activation of inflammatory responses caused by neurotoxic factors such as nitric oxide (NO), tumour necrosis factor-alpha (TNFα), interferon gamma (IFNγ), interleukin-6 (IL-6) and interleukin-1β (IL-1β) which damage adjacent neurons [9-13]. Evidence supporting the potential role of microglia-mediated neuroinflammation in CM was further provided by our recent study which showed that a by-product of haemoglobin metabolism by the malarial parasite, hemozoin induced neuroinflammation in BV-2 microglia [14]. Consequently, pharmacological modulation of neuroinflammation is a potential strategy in the adjunctive treatment of the neurological sequelae in CM.

In recent years, investigations have been focusing on anti-inflammatory natural products due to their potential in treating neurodegenerative disorders. In fact, there is an increasing body of research data showing that anti-inflammatory and

neuroprotective natural products from plants are potential sources of therapeutic small molecules for the amelioration and prevention of neurodegeneration observed in some neurodegenerative and neurological disorders.

Zanthoxylum zanthoxyloides (Lam.) Zepern. & Timler (Rutaceae) is a medicinal plant commonly used in the treatment of sickle cell disease, malaria, stomach ache, toothache, coughs, urinary and venereal diseases, leprous ulcerations, rheumatism, and lumbago [15-17]. Extracts of *Z zanthoxyloides* have been reported to demonstrate a number of pharmacological activities, including antiplasmodial [18,19] and anti-sickling [20,21] properties.

The first report suggesting the anti-inflammatory activity of *Z zanthoxyloides* was published by Oriowo [22]. In that study, *Z zanthoxyloides* showed inhibition of carrageenan-induced rat paw oedema and prostaglandin synthesis. *In vivo* anti-inflammatory activity of this plant was further confirmed by Prempeh and Mensah-Attipoe [23]. In this study, we report the effects of *Z zanthoxyloides* root extract on neuroinflammation in BV-2 microglia stimulated with lipopolysaccharide (LPS) and synthetic hemozoin. We have also used bioactivity-guided fractionation to identify skimmianine as an anti-neuroinflammatory compounds in the root extract of this plant.

Materials and methods

Plant material and extraction

The roots of *Zanthoxylum zanthoxyloides* (Lam.) Zepern. & Timler were collected in the botanical garden of University of Ibadan, Nigeria in the month of June 2015. The plant material was authenticated by Mr D.P.O. Esimekhuai, a taxonomist in the Department of Botany Herbarium, University of Ibadan, Nigeria where a voucher specimen (UIH 22474) was deposited.

The powdered plant material (288 g) was Soxhlet extracted sequentially in *n*-hexane, dichloromethane and methanol (800 mL each). The methanol extract was filtered and concentrated using a rotary evaporator. The dried extract was suspended in DMSO for pharmacological studies. The final concentration of DMSO in cell culture was 0.2%. BV-2 microglia were stimulated with bacterial lipopolysaccharide (LPS)

from *S. typhimurium* (Innaxon) or synthetic hemozoin (InvivoGen) to induce neuroinflammation.

Cell culture

BV-2 mouse microglia cell line (ICLCATL03001) was purchased from Interlab Cell Line Collection (Banca Biologica e Cell Factory, Italy) and cultured in RPMI medium supplemented with 10% foetal bovine serum. HT-22 mouse hippocampal neuronal cells were a kind gift from Dr Jeff Davis (Swansea University, UK). The cells were cultured in DMEM supplemented with 10% foetal bovine serum. Human Embryonic Kidney (HEK293) cells were purchased from the European Collection of Cell Cultures (ECACC). They were cultured in minimum essential medium (MEM) (Gibco) supplemented with 10% foetal bovine serum. All cells were maintained at 37°C in 5% CO_2. Cells were seeded out at 2 x 10^5 cells/ml in each well of culture plates for all pharmacological experiments.

Determination of BV-2 cell viability

Viability of BV-2 cells stimulated with either LPS or hemozoin in the presence or absence of *Z. zanthoxyloides* was measured by 3-(4, 5-dimethylthiazol-2-yl)-2, 5-diphenyl tetrazolium bromide (MTT) assay. Cells were treated with *Z. zanthoxyloides* (4, 6 and 8µg/ml) for 30 min and then incubated with either LPS (100 ηg/ml) or hemozoin (400 µg/ml) for 24 h. Then cell culture medium was removed and replaced with MTT solution (5 mg/ml), followed by incubation for 4 h. Thereafter, 150 μL of MTT solution was removed from each well and replaced with 150 μL DMSO. Formazan crystals were dissolved by shaking the plate on a rocker. Absorbance was read in a microplate reader (Infinite F50, Tecan) at a wavelength of at 570nm.

Measurement of NO, PGE_2, TNFα, IL-6 and IL-1β in culture supernatants

Cultured BV-2 microglia were treated with *Z. zanthoxyloides* (4, 6 and 8 μg/ml) for 30 min, followed by stimulation with either LPS (100 ng/ml) or hemozoin (400 μg/ml) for a further 24 h. Culture supernatants were collected, and levels of NO were determined using the Griess assay kit (Promega). Levels of PGE_2 were detected using the PGE_2 enzyme immunoassay (EIA) kit (Arbor Assays). Levels of TNFα, IL-6, IL-1β and IL-10 were measured with mouse ELISA assay kits (Biolegend). Levels of pro-IL-1β were measured using mouse pro-IL-1β ELISA kit (Thermo Scientific). All

ELISA measurements were carried out according to the manufacturer's instructions and absorbance measured at 450 nm in a Tecan F50 microplate reader.

PathScan® MAPK multi-target sandwich ELISA

Experiments were carried out to investigate effects of *Z. zanthoxyloides* (4, 6 and 8 μg/ml) on protein levels of phospho-p38, phospho-JNK and phospho-ERK1/2 in BV-2 cells stimulated with either LPS (100 ng/ml) or hemozoin (400 μg/ml) for 60 min. Following inflammatory stimulation, cells were washed with cold phosphate-buffered saline (PBS) and lysed with lysis buffer (Cell Signalling Technology). Cell lysates were analysed as earlier described [24], using PathScan® MAP Kinase Multi-Target Sandwich ELISA for phospho-p38, phospho-ERK1/2 and phospho-JNK, according to the manufacturer's instructions (Cell Signalling Technology). Absorbance was measured at 450 nm in a Tecan F50 microplate reader.

Immunoblotting

Cells were treated with *Z. zanthoxyloides* (4, 6 and 8 μg/ml) for 30 min, followed by stimulation with either LPS (100 ng/ml) or hemozoin (400 μg/ml) for different time points to evaluate effects on different proteins. To achieve this, immunoblotting was carried out on 20-40 μg of protein lysates from cells. These were subjected to sodium dodecyl sulfate–polyacrylamide gel electrophoresis (SDS-PAGE), followed by transfer onto polyvinylidene fluoride (PVDF) membranes (Millipore). Following incubation of membranes with blocking reagent at room temperature for 1 h, they were further incubated with primary antibodies overnight at 4°C. Primary antibodies used were rabbit anti-COX-2 (1:1000; Abcam), rabbit anti-iNOS (1:1000; Cell Signaling Technology), rabbit anti-IκBα (1:500; Santa Cruz Biotechnology), rabbit anti-phospho-IκBα (1:500; Santa Cruz Biotechnology), rabbit anti-phospho-p65 (1:500; Abcam), rabbit anti-caspase-1 (1:500; Santa Cruz Biotechnology), rabbit anti-NLRP3 (1:1000; Abcam), rabbit anti-p38 (1:500; Santa Cruz Biotechnology), rabbit anti-phospho-p38 (1:1000; Cell Signaling Technology), and rabbit anti-actin (1:1000; Sigma). Membranes were then washed (15 min; 3 times) in tris-buffered saline + Tween 20 (TBS-T), followed by incubation with Alexa Fluor 680 goat anti-rabbit secondary antibody (1:10000; Thermo Scientific) at room temperature for 1 h. Blots were detected using a Licor Odyssey Imager. All Western blot experiments were carried out at least three times and blots quantified using the image J software.

NF-κB luciferase reporter gene assay

The production of pro-inflammatory mediators in neuroinflammation is controlled by NF-κB through its transcriptional activity. In order to evaluate the effect of *Z. zanthoxyloides* on NF-κB-mediated gene transcription, we carried out a reporter gene assay. Cultured HEK293 cells were seeded out at a concentration of 4×10^5 cells/ml in a solid-white 96-well plate in Opti-MEM reduced serum medium (Gibco). The cells were then transfected with Cignal NF-κB luciferase reporter using lipofectamine 2000 transfection reagent (ThermoFisher) and incubated for 16 h in 5% CO_2 incubator at 37ºC. Thereafter, transfected cells were treated with *Z. zanthoxyloides* (4, 6, and 8 μg/ml) 30 min prior to stimulation with TNFα (1 ng/ml) for a further 6 h. Luciferase activity was measured with Dual-Glo luciferase assay kit (Promega, UK). Luminescence was measured using FLUOstar OPTIMA microplate reader (BMG LABTECH).

NF-κB p65 DNA binding assay

DNA binding capacity of NF-κB following activation by either LPS or hemozoin was quantitatively evaluated using the ELISA-based TransAM® NF-κB transcription factor kit (Active Motif). This kit contains a 96-well plate to which an oligonucleotide containing the NF-κB consensus site (5'-GGGACTTTCC-3') has been immobilised. Following treatment of BV-2 microglia with *Z. zanthoxyloides* (4, 6 and 8 μg/ml) for 30 min, the cells were stimulated with either LPS (100 ng/ml) or hemozoin (400μg/ml) for 60 min. This was followed by preparation of nuclear extracts, which were then used in DNA binding assays according to the manufacturer's instructions. Absorbance was measured at 450nm with a microplate reader (Infinite F50, Tecan).

Caspase-Glo®1 inflammasome assay

The caspase-Glo®1 inflammasome assay (Promega) is an established bioluminescent method to selectively measure the activity of caspase-1 directly in live cells. This assay was used to evaluate the effect of *Z. zanthoxyloides* extract on caspase-1 activity in BV-2 microglia stimulated with hemozoin. BV-2 cells were seeded in 96-well plates and pre-treated with *Z. zanthoxyloides* (4, 6 and 8 μg/ml) 30 min prior to activation with hemozoin (400 μg/ml) for a further 24 h. Activity of caspase-1 in cells was thereafter measured according to the manufacturer's

instructions. Luminescence was read with FLUOstar OPTIM reader (BMG LABTECH).

Transwell co-culture of BV-2 microglia and HT-22 neurons

The effects of *Z. zanthoxyloides* on neuroinflammation-mediated neuronal damage was investigated using a transwell co-culture system. BV-2 cells were cultured at a density of 5×10^4 on transwell inserts (pore size 0.4 µm; Corning) in a 6-well plate placed above the HT-22 layer. Twenty-four hours after establishing co-culture, BV-2 cells were pre-treated with *Z. zanthoxyloides* (4, 6 and 8 µg/ml) and then stimulated with LPS (1 µg/ml) for 24 h. After the experiment, the viability of HT-22 neurons was evaluated using the CyQUANT™ LDH cytotoxicity assay (Invitrogen), according to the manufacturer's instructions. Intracellular generation of reactive oxygen species (ROS) in HT-22 neurons was determined using the DCFDA-cellular reactive oxygen species detection assay kit, (Abcam).

Culture supernatants were collected and analysed for levels of NO, TNFα, IL-6, using mouse ELISA kits (Biolegend).

Statistical analyses

Values of all experiments were represented as a mean ± SEM of at least 3 experiments. Data were analysed using one-way ANOVA followed by a post hoc Tukey test. Statistical difference of p value less than 0.05 ($p<0.05$) were considered significant.

Results

Effects of the extract of *Z. zanthoxyloides* on the release of pro- and anti-inflammatory cytokines in activated BV-2 microglia

In experiments to determine the effects of. *Z. zanthoxyloides* extract on pro-inflammatory cytokines, stimulation of BV-2 microglia with LPS resulted in significant ($p<0.001$) elevation in the levels of TNFα (Figure 1A), IL-6 (Figure 1B) and IL-1β (Figure 1C), when compared with control (unstimulated) cells. On the other hand, LPS stimulation produced a significant ($p<0.001$) reduction in the anti-inflammatory cytokine IL-10 (Figure 1D). However, in BV-2 microglia treated with 4, 6 and 8 µg/ml of *Z. zanthoxyloides* extract prior to stimulation with LPS, significant ($p<0.05$) and concentration-dependent reduction in the secretion of TNFα, IL-6 and IL-1β, were

observed while the production of IL-10 was increased in comparison with cells stimulated with LPS alone (Figures 1A-D).

In the presence of hemozoin (400 μg/ml), there were significant ($p<0.001$) increases in the secretion of TNFα (Figure 2A), IL-6 (Figure 2B), pro-IL-1β (Figure 2C), and IL-1β (Figure 2D) in BV-2 microglia. This was accompanied by a reduction in the levels of IL-10 (Figure 2E). At the lowest concentration (4 μg/ml) of *Z. zanthoxyloides* investigated, there was a suppression of hemozoin-induced increased production of TNFα, pro-IL-1β and IL-1β in BV-2 cells. Interestingly, this concentration of the extract did not produce significant reduction in IL-6. Increasing the concentrations of the extract to 6 and 8 μg/ml, there were reductions in the secretion of all the pro-inflammatory cytokines analysed (Figures 2A-D). Pre-treatment of hemozoin-stimulated BV-2 microglia with *Z. zanthoxyloides* (4, 6 and 8 μg/ml) prevented reduction in IL-10 levels in the cells (Figure 2E). Results of MTT assays revealed that treatment of BV-2 microglia stimulated with either LPS or hemozoin did not cause a reduction in cell viability (Figures 3A and 3B).

Z. zanthoxyloides extract suppressed iNOS-mediated NO production in activated BV-2 microglia

In experiments to further evaluate the effects of *Z. zanthoxyloides* on neuroinflammation, it was observed that at 4, 6 and 8 μg/ml of the extract, there was a significant ($p<0.01$) and concentration-dependent reduction in both LPS-induced NO production (Figure 4A) and elevated iNOS protein levels (Figures 4B and 4C) in BV-2 microglia.

Similarly, figure 5A shows that stimulation of BV-2 microglia caused an increase in the production of NO, which was then significantly ($p<0.01$) reduced in the presence of *Z. zanthoxyloides* (4, 6 and 8 μg/ml). This was accompanied by a concentration-dependent and significant reduction in iNOS protein (Figures 5B and 5C).

Z. zanthoxyloides extract reduced PGE_2 production in activated BV-2 microglia through COX-2 inhibition

LPS stimulation of BV-2 microglia revealed a significant increase in the production of PGE_2 (Figure 6A), as well as an elevation in protein expression of COX-2 in comparison with unstimulated cells (Figures 6B and 6C). However, pre-treatment of

the cells with 4 μg/ml of *Z. zanthoxyloides* did not produce significant reduction in PGE_2 production but caused a significant ($p<0.01$) decrease in COX-2 protein, in comparison with cells stimulated with LPS alone. In the presence of 6 and 8 μg/ml of the extract, LPS-induced increase in PGE_2 production and COX-2 protein expression were significantly ($p<0.01$) reduced (Figures 6A and 6B). Similar reductions in PGE_2 production and COX-2 protein levels were observed in hemozoin-stimulated BV-2 microglia which were pre-treated with *Z. zanthoxyloides* (4, 6 and 8μg/ml) (Figures 7A-C).

Effect of *Z. zanthoxyloides* on NF-κB-dependent gene expression in HEK293 cells

Following observations revealing inhibition of neuroinflammation in LPS- and hemozoin-stimulated BV-2 microglia by *Z. zanthoxyloides,* we sought to understand any roles played by the NF-κB transcription factor in these actions. Firstly, we investigated the effects of the extract on NF-κB-dependent gene expression in general. To achieve this, a plasmid construct bearing a luciferase reporter gene under the control of NF-κB was transiently transfected into HEK293 cells. Stimulation of the cells with TNFα resulted in activation of the NF-κB-driven luciferase expression (Figure 8), and was significantly ($p<0.001$) reduced by *Z. zanthoxyloides* in a concentration-dependent manner (Figure 8).

Inhibition of neuroinflammation by *Z. zanthoxyloides* in activated BV-2 microglia is mediated through NF-κB

Thereafter, the specific effects of *Z. zanthoxyloides* on protein targets in the NF-κB signalling pathway following stimulation with LPS and hemozoin were investigated in BV-2 microglia. Figures 9A-9H show that pre-treatment of the cells with *Z. zanthoxyloides* (4, 6 and 8 μg/ml) prior to stimulation with LPS or hemozoin caused a significant ($p<0.05$) and concentration-dependent reduction in the levels of both phospho-IκB and phospho-p65 proteins.

Interestingly, a significant prevention of LPS-induced degradation of IκB was only observed with 8 μg/ml of the extract (Figures 10A and 10B) at all concentrations of the extract investigated, whereas hemozoin-induced degradation of IκB was significantly attenuated at 4, 6 and 8 μg/ml of the extract (Figures 10C and 10D).

In transcriptional factor assays to determine whether *Z. zanthoxyloides* had any effect on DNA binding of NF-κB in BV-2 microglia following stimulation with LPS (100 ng/ml) or hemozoin (400 μg/ml), it was observed that treatment with 4 μg/ml of the extract did not produce significant inhibition of DNA binding in cells stimulated with LPS (Figure 11A) or hemozoin (Figure 11B). However, significant reduction in DNA binding activity of NF-κB by *Z. zanthoxyloides* was observed at 6 and 8 μg/ml concentrations of the extract (Figures 11A and B).

Z. zanthoxyloides inhibits activation of p38 MAP kinase in LPS-activated BV-2 microglia

In order to explore whether *Z. zanthoxyloides* extract inhibit neuroinflammation by targeting the MAP kinases, we carried out an ELISA experiment to investigate its effects on the levels of phospho-p38, phospho-JNK and phopspho-p42/44 proteins following stimulation of BV-2 microglia with LPS. Results showed that the extract significantly reduced ($p<0.01$) LPS-induced elevated levels of phospho-p38, but not phospho-JNK or phospho-p42/44 MAP kinases (Supplementary Data 4A, 4B and 4C). Reduction of LPS-induced p38 MAP kinase activation in BV-2 microglia by *Z. zanthoxyloides* extract (4, 6 and 8 μg/ml) was further confirmed with immunoblotting (Figures 12A and B).

Z. zanthoxyloides targets NLRP3inflammasome/caspase-1 activation in hemozoin-stimulated BV-2 microglia

Following our observation showing that *Z. zanthoxyloides* reduced the production of both pro-IL-1β and IL-1β in hemozoin-activated BV-2 microglia, we were interested in further investigating any modulation of NLRP3 activation by the extract. Results in figure 13 show that stimulation of BV-2 microglia with hemozoin (400 μg/ml) resulted in an increase in protein expression of NLRP3, in comparison with unstimulated cells. On pre-treating the cells with *Z. zanthoxyloides* extract (4, 6 and 8 μg/ml) prior to hemozoin stimulation, a significant ($p<0.05$) and concentration-dependent reduction in NLRP3 protein expression was observed (Figure 13). Hemozoin stimulation also produced significant ($p<0.001$) elevation in caspase-1 activity in BV-2 cells. In the presence of *Z. zanthoxyloides*, hemozoin-mediated elevated caspase-1 activity in BV-2 microglia was significantly ($p<0.05$) reduced as shown by lower levels of bioluminescence (Figure 14A). Interestingly, *Z. zanthoxyloides* also

produced significant ($p<0.001$) reduction in hemozoin-induced increase in caspase-1 expression in BV-2 cells (Figures 14B and 14C).

Pre-treatment with *Z. zanthoxyloides* extract protected HT-22 neurons from microglia-mediated toxicity

Having established that *Z. zanthoxyloides* extract inhibited neuroinflammation in BV-2 microglia, we were interested in investigating whether the extract could reduce microglia-mediated neuronal damage. Stimulating the microglia layer of a BV-2 microglia-HT-22 neuron transwell co-culture resulted in a significant ($p<0.001$) increase in LDH released from the neurons, indicating a reduction in viable cells (Figure 15A). Treating microglia with 4 μg/ml of *Z. zanthoxyloides* did not have significant effect on microglia-mediated neurotoxicity. However, with higher concentrations of the extract (6 and 8 μg/ml), statistically significant ($p<0.05$) reduction in LDH release was observed, suggesting reduced neurotoxicity (Figure 15A).

Stimulation of the microglia layer with LPS also resulted in a significant increase ($p<0.001$) in generation of ROS in HT-22 neurons, in comparison with cells which were co-cultured with unstimulated microglia (Figure 15B). When the microglia layer was pre-treated with *Z. zanthoxyloides* (4, 6 and 8 μg/ml) prior to LPS stimulation, neuronal generation of ROS was significantly ($p<0.05$) reduced (Figure 15B).

In order to confirm the roles of excessive inflammatory mediator release in neuronal viability, we analysed supernatants obtained from the co-culture and demonstrated that stimulation with LPS (1μg/ml) resulted in significant ($p<0.001$) increases in the concentrations of NO (Figure 16A), TNFα (Figure 16B) and IL-6 (Figure 16C). In the presence of *Z. zanthoxyloides* (4, 6 and 8 μg/ml), LPS-induced NO production in the co-culture was significantly reduced ($p<0.05$), in a concentration-dependent manner (Figure 16A). Interestingly, in the co-culture pre-treated with *Z. zanthoxyloides* (4 μg/ml) secretion of TNFα was not significantly reduced, in compassion with LPS stimulation (Figure 16B). With higher concentrations of *Z. zanthoxyloides* (6 and 8 μg/ml), TNFα concentrations were significantly ($p<0.05$) reduced (Figure 16B). LPS-induced elevation in the levels of IL-6 in the co-culture were significantly reduced ($p<0.05$) on pre-treatment with 4, 6 and 8 μg/ml of *Z. zanthoxyloides* prior to LPS (Figure 16C).

Bioactivity-guided isolation of skimmianine from *Z. zanthoxyloides*

The methanol extract of *Z. zanthoxyloides* was subjected to solid phase extraction using a Strata C-18 cartridge 20 g (Phenomenex). The cartridge was previously washed with 50 mL of methanol, and followed by running 100 mL of water. The extract (2 g) was dissolved in 10 ml of 10% methanol in water. The cartridge was eluted with a gradient of MeOH-water mixture to obtain four fractions (**FR1**, 20:80; **FR2**, 50:50; **FR3**, 80:20 and **FR4**, 100:0).

FR1 (4, 6 and 8 μg/ml), **FR2** (4, 6 and 8 μg/ml), **FR3** (4, 6 and 8 μg/ml) and **FR4** (4, 6 and 8 μg/ml) were evaluated for anti-inflammatory activity on TNFα production in LPS-stimulated BV-2 microglia. **FR3** showed the highest bioactivity in reducing LPS-induced TNFα production without affecting viability in BV-2 microglia (Supplementary Data 1A and 1B).

FR3 (26 mg) was purified on an Agilent 1260 infinity HPLC System equipped with an Agilent 1260 DAD and an Ace-5 C18 column (150 × 21.2 mm, 5 μm particle size, Hichrom Ltd). Preparative HPLC was performed using a gradient of mobile phase A (water with 0.1% trifluoroacetic acid) and mobile phase B (methanol with trifluoroacetic acid) with the following time schedule: 30% B, 0–35 min; 100% B, 35-37 min; 100% B, 37-39 min; 30% B, 39-42 min. The flow rate was maintained at 10.0 mL/min and UV absorbance was recorded at 254, 280 and 310 nm. Preparative HPLC was used to purify **FR3** and the chromatogram showed the main compound at 17.596 min as the retention time (Figure 17).

Nuclear magnetic resonance and mass spectrometry

The structure of compound isolated from **FR3** was determined using spectroscopic analyses which included proton (^{1}H) and carbon (^{13}C) NMR while 2D NMR experiments were ^{1}H-^{1}H COSY (Correlation SpectroscopY), HMBC (^{1}H-^{13}C Heteronuclear Multiple Bond Correlation Spectroscopy) and HSQC (^{1}H-^{13}C Heteronuclear Single Quantum correlation). Experiments were performed on either a Bruker AMX 600 or a Bruker AMX 300 instrument (Bruker, Germany). NMR data revealed **FR3** to be skimmianine with a molecular formula, $C_{14}H_{13}NO_4$ (Figure 18A, B and C).

High resolution mass spectra were recorded at the National Mass Spectrometry Facility, Swansea, UK on a LTQ Orbitrap XL1 spectrometer. The analytes were

prepared in methanol and the mass spectrum was analysed relating their mass to charge (m/z) ratio. HR-MS mass spectrum confirmed the molecular weight of skimmianine (Figure 18D).

Discussion

Chronic inflammation in the brain has been implicated in the pathobiology of a number neurodegenerative disorders, as well as in neurological dysfunction accompanying some parasitic diseases such as cerebral malaria. This has created opportunities to identify anti-inflammatory natural products as therapeutic potentials for disorders which are linked to neuroinflammation [25]. Our investigations in this study have shown that an extract from the roots of *Z. zanthoxyloides* inhibited neuroinflammation in LPS-activated BV-2 microglia by reducing elevated levels of pro-inflammatory cytokines TNFα, IL-6 and IL-1β while increasing levels of the anti-inflammatory cytokine IL-10. Further experiments showed that the extract prevented microglia-mediated damage to mouse hippocampal HT-22 neurons. Investigations have shown that in neurodegenerative disorders like AD, activation of microglia by LPS is termed M1 or classical activation, and is accompanied by excessive release of pro-inflammatory cytokines, such as IL-1β, TNFα, STAT3, and IL-6 resulting in neuronal loss [26]. On the other hand, the alternative M2 anti-inflammatory phenotype is associated with the release of high levels of anti-inflammatory cytokines such as IL-10 [27]. It is believed that the phenotype switches from M2 to M1 in the course of AD, with resulting neuronal damage [26]. This is the first report showing that *Z. zanthoxyloides* is potentially capable of blocking the pro-inflammatory phenotype while enhancing the anti-inflammatory phenotype of the microglia, thus suggesting a potential role for secondary metabolites in this plant for the treatment of AD and similar neurodegenerative pathologies.

Microglia-mediated neuronal death is due to the long-term impact of excessive nitrogen species, which contribute significantly to apoptotic death through irreversible nitrosative injury to neurons [28]. Excessive production of iNOS-generated NO is therefore a critical process in neuroinflammation. We further demonstared anti-inflammatory activity of *Z. zanthoxyloides* by demonstrating its suppressive effect of NO production in LPS-activated microglia through inhibition of iNOS protein expression. Furthermore, COX-2-mediated PGE_2 released from LPS-activated

microglia has been strongly implicated in neurodegeneration [29]. Our experiments showed that *Z. zanthoxyloides* suppressed PGE_2 production in LPS-activated microglia through the reduction of COX-2 protein expression, which further confirms inhibition of neuroinflammation by this plant.

A study reported by Oriowo [22] first suggested that *Z. zanthoxyloides* produced anti-inflammatory property. This study showed that an extractive from this plant reduced carrageenan-induced paw oedema in rats through mechanisms related to inhibition of prostaglandin synthesis. Similar observations were made in a study reported by Prempeh and Mensah-Attipoe [23]. The results obtained in this study have shown that mechanisms involving suppression of NO/iNOS and the pro-inflammatory cytokine production also contribute to the anti-inflammatory activity of *Z. zanthoxyloides,* at least in BV-2 microglia, which are brain-resident macrophages.

Data showing that *Z.zanthoxyloides* produced marked inhibition of neuroinflammation in LPS-activated BV-2 microglia prompted a further investigation into the possible mechanism(s) involved in this action. Based on the established regulatory role of the NF-κB transcription factor in the genes encoding pro-inflammatory cytokines such as TNFα, IL-6 and IL-1β, as well as pro-inflammatory proteins such as iNOS and COX-2 in the microglia [30,31], we next explored the effects of *Z. zanthoxyloides* on NF-κB signalling pathway. This objective was driven by evidence showing that LPS-induced activation of NF-κB pathway is initiated by a number of upstream processes which results in the phosphorylation of IκB by IκB kinase (IKK), resulting in ubiquitination of IκB by ubiquitin ligases and its degradation by the 26S proteasome, followed by the release of NF-κB and its translocation to the nucleus [32-34].

Initial experiments showed that *Z. zanthoxyloides* inhibited NF-κB-mediated gene expression in HEK293 cells that were transiently transfected with a plasmid construct bearing a luciferase reporter gene. Consequently, we proceeded to examine the effects of the extract on individual steps of NF-κB activation in LPS-activated BV-2 microglia. *Zanthoxylum zanthoxyloides* reduced LPS-induced NF-κB activation in BV-2 microglia by suppressing p65 phosphorylation and/or degradation of IκBα, and the subsequent DNA binding of p65 sub-unit. We therefore propose that these

effects possibly account for the reduction of LPS-induced production of pro-inflammatory mediators by the extract in BV-2 microglia.

Accumulating evidence suggests that elevated the mitogen activated protein (MAP) kinases contribute to neuroinflammation [35]. The mammalian MAPKs include c-Jun NH2-terminal kinase (JNK), p38 MAPK, and extracellular signal-regulated kinase (ERK), and known to regulate various cellular activities including proliferation, differentiation, apoptosis or survival, inflammation, and innate immunity [36]. We therefore next explored the effects of *Z. zanthoxyloides* extract on the activation of the MAPKs in LPS-activated microglia, and showed that the extract was effective against LPS-induced activation of p38 MAPK, but not JNK or ERK. This outcome further demonstrates the anti-inflammatory activity *Z. zanthoxyloides,* through inhibition of p38 MAPK inhibition. This outcome was not unexpected; of the MAPKs, the p38 MAPK has been strongly linked to neuroinflammation [37]. In fact, p38-mediated production of NO and TNFα in LPS-activated primary rat and human microglia have been shown in studies [38,39]. Furthermore, p38 inhibitors reduced neuroinflammation in BV-2 microglia and in mice [40,41]. Selective inhibition of p38 activation in BV-2 microglia by *Z. zanthoxyloides* needs further investigation; this may result in the identification of a novel natural inhibitor of the p38 MAP kinase.

Hemozoin produced by *Plasmodium falciparum* during malaria infection is now known to induce inflammation in peripheral macrophages [42] and in BV-2 microglia [14] to release inflammatory mediators. Interestingly, *Z. zanthoxyloides* is used locally in the treatment of malaria, and in fact has been shown to produce antimalarial activity *in vitro* [43]. We were therefore interested in investigating the effects of the plant extract on hemozoin-induced inflammation in BV-2 microglia.

Similar to results obtained in experiments on LPS-activated BV-2 microglia, experiments revealed that *Z. zanthoxyloides* prevented neuroinflammation in BV-2 microglia stimulated with synthetic hemozoin by reducing production of TNFα, IL-6 and increasing levels of IL-10. The extract also suppressed iNOS-mediated production of NO, as well as COX-2-mediated PGE_2 production in hemozoin-stimulated BV-2 microglia. These results seem to suggest that natural products from *Z. zanthoxyloides* could be important therapeutic adjuvants in the treatment of cerebral malaria.

A striking feature of the activity of *Z. zanthoxyloides* on hemozoin-induced neuroinflammation is the reduction in both pro-IL-1β and IL-1β production. It has been established that the production of IL-1β following stimulation of BV-2 microglia is downstream of NLRP3 inflammasome activation [14]. It was also proposed that hemozoin is able to activate NLRP3, which in turn results in the activation of caspase-1, and the cleavage of pro- IL-1β to generate IL-1β [44]. We showed that the extract of *Z. zanthoxyloides* produced inhibitory effect on hemozoin-induced increase in caspase-1 activity and NLRP3 inflammasome protein levels, suggesting a role for this pathway in the anti-inflammatory activity of the extract in BV-2 microglia. To our knowledge, this is the first study reporting inhibition of hemozoin-induced neuroinflammation by a plant extract.

Remarkably, *Z. zanthoxyloides* also suppressed hemozoin-induced increased expression of phospho-p65, while preventing phosphorylation and degradation of IκB, as well as DNA binding of NF-κB in BV-2 microglia. The dual effects of *Z. zanthoxyloides* on NLRP3 inflammasome and NF-κB activation in hemozoin-activated BV-2 microglia could be due to its effects on cross-talk mechanisms between NF-κB and NLRP3 in innate immunity [14,45].

The encouraging results showing marked anti-neuroinflammatory activity by the root extract of *Z. zanthoxyloides* encouraged us to conduct a bioactivity-guided isolation of skimmianine from the extract. Skimmianine is the most abundant furoquinoline alkaloid that has been isolated from different parts of *Zanthoxylum* species [46,47]. Skimmianine has been previously shown to produce anti-inflammatory against carrageenan-induced rat paw oedema, accompanied by a reduction in the mRNA levels of TNF-α and IL-6, as well as production of NO and PGE_2 [48]. Also, a study reported by Yoon et al. showed that this alkaloid reduced NO production in LPS-stimulated BV-2 microglia [49]. The effects of skimmianine on neuroinflammation in the microglia needs to be explored with a view to identifying its contribution to the anti-neuroinflammatory activity of *Z. zanthoxyloides.*

In summary we have shown that the root extract of *Z. zanthoxyloides* inhibited neuroinflammation in BV-2 microglia stimulated with both LPS and synthetic hemozoin. We also provide evidence supporting inhibition of p38 MAPK activation by *Z. zanthoxyloides,* which may be one of the molecular mechanisms of the anti-

inflammatory action of the plant. We further showed that the plant extract targets NF-κB activation pathway to produce anti-inflammatory activity against both LPS and hemozoin, in addition to blocking NLRP3 inflammasome activation to suppress hemozoin-induced production of IL-1β. Bioassay-guided fractionation of the extract revealed skimmianine as an anti-inflammatory constituent in the plant. Further studies will investigate the molecular mechanisms involved in the anti-neuroinflammatory acivity of skimmianine in the microglia.

Acknowledgements

Folashade Ogunrinade was funded by the Schlumberger Foundation through the Faculty for the Future Fellowship. Idowu Akande received a Travel Grant (Needs Assessment Intervention Fund) from the University of Lagos, Nigeria.

Conflict of interest

There are no known conflicts of interest associated with this publication and there has been no financial support for this work that could have influenced its outcome.

CRediT author statement

Folashade A Ogunrinade: Investigation. **Stephanie T Guetchueng:** Investigation. **Folashade O Katola:** Investigation. **Mutalib A Aderogba**: Investigation. **Idowu S. Akande:** Investigation**. Satyajit D Sarker**: Conceptualisation, Methodology, Writing - Review & Editing, Supervision, Project administration. **Olumayokun A Olajide:** Conceptualisation**,** Methodology**,** Writing - Original Draft, Writing - Review & Editing, Supervision, Project administration.

References

1. Ransohoff RM. How neuroinflammation contributes to neurodegeneration. *Science* 2016; **353**: 777-783.
2. Varnum MM, Ikezu T. The classification of microglial activation phenotypes on neurodegeneration and regeneration in Alzheimer's disease brain. *Arch Immunol Ther Exp* (Warsz) 2012; **60**: 251–266.
3. Calsolaro V, Edison P. Neuroinflammation in Alzheimer's disease: Current evidence and future directions. *Alzheimer's Dement* 2016; **12**: 719-732.
4. Guo JT et al. Inflammation-dependent cerebral deposition of serum amyloid a protein in a mouse model of amyloidosis. *J Neurosci* 2002; **22**: 5900–5909.
5. Hirsch EC et al. Neuroinflammation in Parkinson's disease. *Parkinsonism Relat Disord.* 2012; **18**, S210-S212.
6. Gelders G et al. Linking neuroinflammation and neurodegeneration in Parkinson's disease. *J Immunol Res.* 2018; **2018**: 4784268.
7. Ioannidis LJ et al. The role of chemokines in severe malaria: more than meets the eye. *Parasitology* 2014; **141**: 602–613.
8. Jaramillo M et al. Hemozoin-inducible pro-inflammatory events *in vivo*: potential role in malaria infection. *J Immunol* 2004; **172**: 3101–3110.
9. Brown H et al. Cytokine expression in the brain in human cerebral malaria. *J Infect Dis* 1999; **180**: 1742–1746.
10. Grau GE et al. Platelet accumulation in brain microvessels in fatal pediatric cerebral malaria. *J Infect Dis* 2003; **187**: 461–466.
11. Wiese, L et al. Neuronal apoptosis, metallothionein expression and proinflammatory responses during cerebral malaria in mice. *Exp Neurol* 2006; **200**: 216–226.
12. McCall M, Sauerwein RW. Interferon-γ-central mediator of protective immune responses against the pre-erythrocytic and blood stage of malaria. *J Leukoc Biol.* 2010; **88**: 1131–1143.
13. Sahu U et al. Association of TNF level with production of circulating cellular microparticles during clinical manifestation of human cerebral malaria. *Hum Immunol* 2013; **74**, 713–721.
14. Velagapudi, R., et al. Induction of neuroinflammation and neurotoxicity by synthetic hemozoin. *Cell Mol Neurobiol*. 2019; **39**: 1187-1200.

15. Chaaib F et al. Antifungal and antioxidant compounds from the root bark of *Fagara zanthoxyloides. Planta Med*. 2003; **69**: 316-320.
16. Adesina SK. The Nigerian *Zanthoxylum*; chemical and biological values. *Afr J Trad CAM* 2005; **2**: 282-301.
17. Gansané A et al. Antiplasmodial activity and toxicity of crude extracts from alternatives parts of plants widely used for the treatment of malaria in Burkina Faso: Contribution for their preservation. *Parasitol Res* 2010; **106**: 335-340.
18. Kassim OO et al. Inhibition of in-vitro growth of *Plasmodium falciparum* by *Pseudocedrela kotschyi* extract alone and in combination with *Fagara zanthoxyloides* extract. *Trans R Soc Trop Med Hyg*. 2009; **103**: 698-702.
19. Enechi OC et al. Methanol extracts of *Fagara zanthoxyloides* leaves possess antimalarial effects and normalizes haematological and biochemical status of *Plasmodium berghei*-passaged mice. *Pharm Biol*. 2019; **57**: 577-585.
20. Ouattara B et al. Antisickling properties of divanilloylquinic acids isolated from *Fagara zanthoxyloides* Lam. (Rutaceae). *Phytomedicine* 2009; **16**, 125-129.
21. Nurain, I.O., et al. Potential of three ethnomedicinal plants as antisickling agents. *Mol Pharm*. 2017; **14**: 172-182.
22. Oriowo MA. Anti-inflammatory activity of piperonyl-4-acrylic isobutyl amide, an extractive from *Zanthoxylum zanthoxyloides*. *Planta Med*. 1982; **44**: 54-56.
23. Prempeh ABA, Mensah-Attipoe J. 2008. *In vivo* inhibition of Prostaglandin E2 production by crude aqueous extract of the root bark of *Zanthoxylum xanthoxyloides*. *Ghana Medical Journal* 2008; **42**: 85-88.
24. Olajide OA et al. *Picralima nitida* seeds suppress PGE2 production by interfering with multiple signalling pathways in IL-1β-stimulated SK-N-SH neuronal cells. *J Ethnopharmacol.* 2014; **152**: 377-383.
25. Olajide OA, Sarker SD. Anti-inflammatory natural products. Medicinal Natural Products: A Disease-Focused Approach 2020. Academic Press Inc.
26. Wang, et al. Role of pro-inflammatory cytokines released from microglia in Alzheimer's disease. *Ann Transl Med*. 2015; **3**: 136.
27. Czeh M et al. The yin and yang of microglia. *Dev Neurosci* 2011; **33**: 199-209.
28. Yuste JE et al. Implications of glial nitric oxide in neurodegenerative diseases. *Front Cell Neurosci*. 2015; **9**: 322.

29. Yousif NM et al. Activation of EP_2 receptor suppresses poly(i: c) and LPS-mediated inflammation in primary microglia and organotypic hippocampal slice cultures: Contributing role for MAPKs. *Glia* 2018; **66**: 708-724.
30. Shabab T et al. Neuroinflammation pathways: A general review. *Int J Neurosci.* 2017; **127**: 624-633.
31. Ju Hwang C et al. NF-κB as a key mediator of brain inflammation in Alzheimer's disease. *CNS Neurol Disord Drug Targets* 2019; **18**: 3-10.
32. Baldwin AS Jr. The NF-kappa B and I kappa B proteins: new discoveries and insights. *Annu Rev Immunol*. 1996; **14**: 649-683.
33. Ghosh S et al. NF-kappa B and Rel proteins: evolutionarily conserved mediators of immune responses. *Annu Rev Immunol* 1998; **16**: 225-260.
34. Karin M, Ben-Neriah Y. 2000. Phosphorylation meets ubiquitination: the control of NF-[kappa]B activity. *Annu Rev Immunol* 2000; **18**: 621-663.
35. Munoz L, Ammit AJ. 2010. Targeting p38 MAPK pathway for the treatment of Alzheimer's disease. *Neuropharmacology* 2010; **58**: 561-568.
36. Kim EK, Choi EJ. Compromised MAPK signaling in human diseases: an update. *Arch Toxicol*. 2015; **89**: 867-882.
37. Bhat NR et al. Extracellular signal-regulated kinase and p38 subgroups of mitogen-activated protein kinases regulate inducible nitric oxide synthase and tumor necrosis factor-alpha gene expression in endotoxin-stimulated primary glial cultures. *J. Neurosci* 1998; **18**: 1633-1641.
38. Lee YB et al. p38 MAP kinase regulates TNF-α production in human astrocytes and microglia by multiple mechanisms. *Cytokine* 2000; **12**, 874-880.
39. Xing B et al. Pioglitazone inhibition of lipopolysaccharide-induced nitric oxide synthase is associated with altered activity of p38 MAP kinase and PI3K/Akt. *J. Neuroinflammation* 2008; **5**: 4.
40. Gee MS et al. A novel and selective p38 Mitogen-Activated Protein Kinase inhibitor attenuates LPS-induced neuroinflammation in BV2 microglia and a mouse model. *Neurochem Res*. 2018; **43**: 2362-2371.
41. Zhao YW et al. Blocking p38 signaling reduces the activation of pro-inflammatory cytokines and the phosphorylation of p38 in the habenula and reverses depressive-like behaviors induced by neuroinflammation. *Front Pharmacol*. 2018; **9**: 511.

42. Griffith JW et al. Pure hemozoin is inflammatory in vivo and activates the NALP3 inflammasome via release of uric acid. *J Immunol*. 2009; **183**: 5208-5220.
43. Goodman CD et al. Anti-plasmodial effects of *Zanthoxylum zanthoxyloides*. *Planta Med* 2019; **85**: 1073-1079.
44. Olivier M et al. Malarial pigment hemozoin and the innate inflammatory response. *Front Immunol*. 2014; **5**: 25.
45. Kersse, K., et al. NOD-like receptors and the innate immune system: coping with danger, damage and death. *Cytokine Growth Factor Rev* 2011; **22:** 257–276.
46. Queiroz EF et al. New and bioactive aromatic compounds from *Zanthoxylum zanthoxyloides*. *Planta medica* 2006; **72**, 746-750.
47. Guetchueng ST et al. Zanthoamides G-I: Three new alkamides from *Zanthoxylum zanthoxyloides*. *Phytochem Lett* 2018; **26**: 125-129.
48. Ratheesh, M., et al. Anti-inflammatory effect of quinoline alkaloid skimmianine isolated from *Ruta graveolens* L. *Inflamm Res*. 2013; **62**: 367-376.
49. Yoon JS et al. Inhibitory alkaloids from *Dictamnus dasycarpus* root barks on lipopolysaccharide-induced nitric oxide production in BV2 cells. *J Enzyme Inhib Med Chem* 2012; **27**: 490-494.

Figure Legends

Figure 1. *Z. zanthoxyloides* suppressed the release of TNFα (A), IL-6 (B) and IL-1β (C), while increasing production of IL-10 (D) in LPS-activated BV-2 microglia. Cells were pre-treated with 4, 6 and 8 μg/ml *Z. zanthoxyloides* extract, followed by stimulation with LPS (100 ng/ml) for a further 24 h. Values are mean ± SEM for at least 3 independent experiments (*p<0.05; **p<0.01; ***p<0.001, compared with LPS stimulation; one-way ANOVA with post-hoc Tukey test).

Figure 2. *Z. zanthoxyloides* suppressed the release of TNFα (A), IL-6 (B), pro-IL-1β (C), and IL-1β (D), while increasing production of IL-10 (E) in hemozoin-activated BV-2 microglia. Cells were pre-treated with 4, 6 and 8 μg/ml *Z. zanthoxyloides* extract, followed by stimulation with hemozoin (400 μg/ml) for a further 24 h. Values are mean ± SEM for at least 3 independent experiments (*p<0.05; **p<0.01; ***p<0.001, compared with hemozoin stimulation; one-way ANOVA with post-hoc Tukey test).

Figure 3. Treatment of BV-2 microglia with *Z. zanthoxyloides* (4, 6 and 8 μg/ml), followed by 100 ng/ml LPS (A) or 400 μg/ml hemozoin (B) for 24 h did not affect cell viability.

Figure 4. Griess assay showing reduction of NO production (A) and immunoblotting showing inhibition of iNOS protein expression (B) by *Z. zanthoxyloides* extract (4, 6 and 8 μg/ml) in LPS-stimulated BV-2 microglia. Densitometric analysis of iNOS immunoblotting (C). Cells were pre-treated with 4, 6 and 8 μg/ml *Z. zanthoxyloides* extract, followed by stimulation with LPS (100 ng/ml) for a further 24 h. Values are mean ± SEM for at least 3 independent experiments (**p<0.01; ***p<0.001, compared with LPS stimulation; one-way ANOVA with post-hoc Tukey test).

Figure 5. Griess assay showing reduction of NO production (A) and immunoblotting showing inhibition of iNOS protein expression (B) by *Z. zanthoxyloides* extract (4, 6 and 8 μg/ml) in hemozoin-stimulated BV-2 microglia. Densitometric analysis of iNOS immunoblotting (C). Cells were pre-treated with 4, 6 and 8 μg/ml *Z. zanthoxyloides* extract, followed by stimulation with hemozoin (400 μg/ml) for a further 24 h. Values are mean ± SEM for at least 3 independent experiments (**p<0.01; ***p<0.001, compared with hemozoin; one-way ANOVA with post-hoc Tukey test).

Figure 6. Enzyme immunoassay showing reduction of PGE_2 production (A) and immunoblotting showing inhibition of COX-2 protein expression (B) by *Z. zanthoxyloides* extract (4, 6 and 8 μg/ml) in LPS-stimulated BV-2 microglia. Densitometric analysis of COX-2 immunoblotting (C). Cells were pre-treated with 4, 6 and 8 μg/ml *Z. zanthoxyloides* extract, followed by stimulation with LPS (100 ng/ml) for a further 24 h. Values are mean ± SEM for at least 3 independent experiments (**p<0.01; ***p<0.001, compared with LPS stimulation; one-way ANOVA with post-hoc Tukey test).

Figure 7. Enzyme immunoassay showing reduction of PGE_2 production (A) and immunoblotting showing inhibition of COX-2 protein expression (B) by *Z. zanthoxyloides* extract (4, 6 and 8 μg/ml) in hemozoin-stimulated BV-2 microglia. Densitometric analysis of COX-2 immunoblotting (C). Cells were pre-treated with 4, 6 and 8 μg/ml *Z. zanthoxyloides* extract, followed by stimulation with hemozoin (400 μg/ml) for a further 24 h. Values are mean ± SEM for at least 3 independent experiments (**p<0.01; ***p<0.001, compared with hemozoin stimulation; one-way ANOVA with post-hoc Tukey test).

Figure 8. *Z. zanthoxyloides* inhibited NF-κB-mediated gene expression. HEK293 transiently transfected with a firefly luciferase gene driven by a NF-κB-regulated promoter were pre-treated for 30 min with *Z. zanthoxyloides* extract (4, 6 and 8 μg/ml) before activation with TNFα (1 ng/ml) for 6 h. The cells were then analysed for luciferase activity. Values are mean ± SEM for at least 3 independent experiments (***p<0.001, compared with TNFα stimulation; one-way ANOVA with post-hoc Tukey test).

Figure 9. Effects *Z. zanthoxyloides* on phosphorylation of IκB and p65 sub-unit in BV-2 microglia activated with LPS or hemozoin. Pre-treatment with *Z. zanthoxyloides* extract (4, 6 and 8 μg/ml) significantly attenuated LPS- (A and B), and hemozoin- (C and D) induced elevation in phospho-IκBα protein after 60-minute incubation. *Z. zanthoxyloides* extract (4, 6 and 8 μg/ml) reduced protein expression of phospho-p65 in BV-2 microglia stimulated with LPS (E and F), and hemozoin (G and H) for 60 min. Values are mean ± SEM for at least 3 independent experiments (*p<0.05; **p<0.01; ***p<0.001, compared with LPS or hemozoin stimulation; one-way ANOVA with post-hoc Tukey test).

Figure 10. *Z. zanthoxyloides* treatment prevented IκB degradation in LPS-(A and B) and hemozoin- (C and D) stimulated BV-2 microglia following 60 min incubation. Values are mean ± SEM for at least 3 independent experiments (*p<0.05; **p<0.01; ***p<0.001, compared with LPS or hemozoin stimulation; one-way ANOVA with post-hoc Tukey test).

Figure 11. *Z. zanthoxyloides* treatment prevented DNA binding of NF-κB in LPS-(A) and hemozoin- (B) stimulated BV-2 microglia. Following treatment with *Z. zanthoxyloides* (4, 6 and 8 μg/ml) and stimulation with either LPS (100 ng/ml) or hemozoin (400 μg/ml) for a further 60 min, NF-κB transcription factor assays for DNA binding were carried on nuclear extracts from BV-2 microglia. Values are mean ± SEM for at least 3 independent experiments (ns-not significant; **p<0.01; ***p<0.001, compared with LPS or hemozoin stimulation; one-way ANOVA with post-hoc Tukey test).

Figure 12. Immunoblotting showing inhibition of LPS-induced phospho-p38 protein expression in BV-2 microglia by *Z. zanthoxyloides* extract (4, 6 and 8 μg/ml) (A). Densitometric analysis of phospho-p38 immunoblotting (B). Values are mean ± SEM for at least 3 independent experiments (***p<0.001, compared with LPS stimulation; one-way ANOVA with post-hoc Tukey test).

Figure 13. *Z. zanthoxyloides* inhibited the expression NLRP3 inflammasome. Following pre-treatment with *Z. zanthoxyloides* extract (4, 6 and 8 μg/ml) and stimulation of BV-2 microglia with hemozoin (400 μg/ml) for 24 h, cell lysates were subjected to immunoblotting. Values are mean ± SEM for at least 3 independent experiments (*p<0.05; ***p<0.001, compared with hemozoin stimulation; one-way ANOVA with post-hoc Tukey test).

Figure 14. Treatment with *Z. zanthoxyloides* extract (4, 6 and 8 μg/ml) reduced caspase 1 activity (A), and caspase-1 protein expression (B and C) following stimulation of BV-2 microglia with hemozoin for 24 h. Values are mean ± SEM for at least 3 independent experiments (*p<0.05; ***p<0.001, compared with hemozoin stimulation; one-way ANOVA with post-hoc Tukey test).

Figure 15. *Z. zanthoxyloides* extract prevented microglia-mediated neurotoxicity and cellular ROS generation. BV-2 microglia-HT-22 neurons were co-cultured in a transwell system and treated with *Z. zanthoxyloides* (4, 6 and 8 μg/ml) prior to

stimulation with LPS (1 μg/ml) for 24 h. Neuronal viability was determined using LDH assay (A), while generation of intracellular ROS in HT-22 was evaluated using the DCFDA fluorescent assay (B). Values are mean ± SEM for at least 3 independent experiments (ns-not significant; *p<0.05; **p<0.01; ***p<0.001, compared with LPS stimulation; one-way ANOVA with post-hoc Tukey test).

Figure 16. Reduction in the levels of NO (A), TNFα (B) and IL-6 (C) by *Z. zanthoxyloides* in a transwell co-culture of BV-2 microglia and HT-22 hippocampal neurons exposed to LPS (1 μg/ml). NO in supernatants was measured using the Griess assay, while TNFα and IL-6 concentrations were measured using mouse ELISA kits. Values are mean ± SEM for at least 3 independent experiments (ns-not significant; *p<0.05; **p<0.01; ***p<0.001, compared with LPS stimulation; one-way ANOVA with post-hoc Tukey test).

Figure 17. Chromatogram of preparative HPLC on FR3.

Figure 18. Proton (A), carbon (B) and mass spectra (D) for skimmianine isolated from the root of *Z. zanthoxyloides*.

Supplementary Data 1. Effects of Fractions FR1, FR2, FR3 and FR4 from the methanol extract of *Z. zanthoxyloides* on TNFα production (A) and viability (B) of LPS-activated BV-2 microglia. Values are mean ± SEM for at least 3 independent experiments (ns-not significant; ***p<0.001, compared with LPS stimulation; one-way ANOVA with post-hoc Tukey test).

Supplementary Data 2. ELISA showing effects of *Z. zanthoxyloides* extract (4, 6 and 8 μg/ml) on phospho-p38 (A), phospho-JNK (B) and phospho-p42/44 protein levels in LPS-activated BV-2 microglia. (**p<0.01; ***p<0.001, compared with LPS stimulation; one-way ANOVA with post-hoc Tukey test)

Figure 1

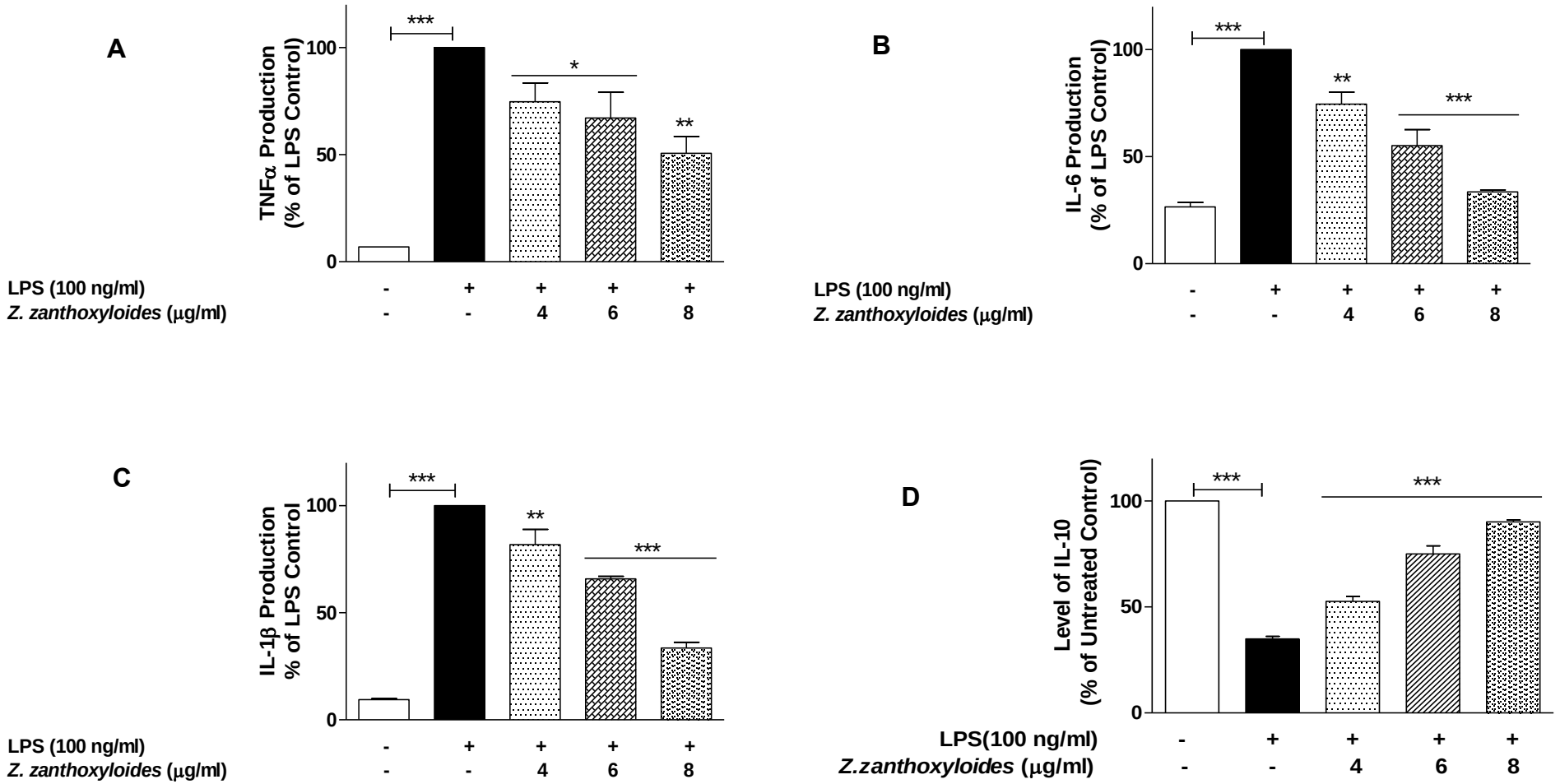
A
TNFα Production
(% of LPS Control)
100
50
0
***
*
**
LPS (100 ng/ml)
Z. zanthoxyloides (μg/ml)
- + + + +
- - 4 6 8
B
IL-6 Production
(% of LPS Control)
100
50
0
***
**
***
LPS (100 ng/ml)
Z. zanthoxyloides (μg/ml)
- + + + +
- - 4 6 8
C
IL-1β Production
% of LPS Control
100
50
0
***
**
***
LPS (100 ng/ml)
Z. zanthoxyloides (μg/ml)
- + + + +
- - 4 6 8
D
Level of IL-10
(% of Untreated Control)
100
50
0
***
***
LPS(100 ng/ml)
Z.zanthoxyloides (μg/ml)
- + + + +
- - 4 6 8

Figure 2

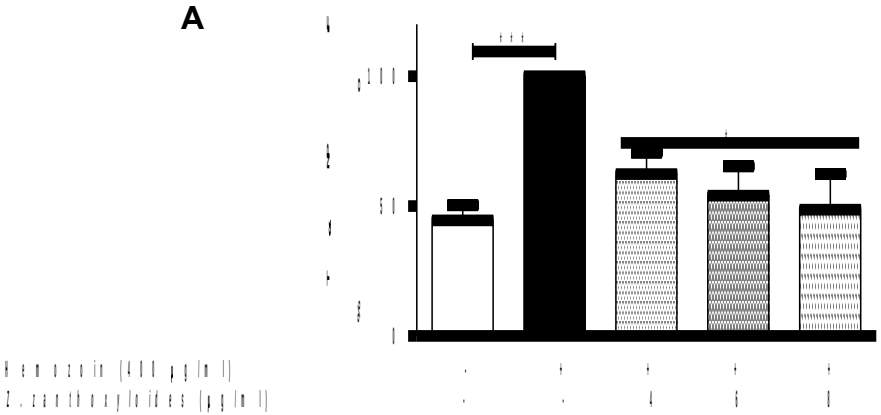
A

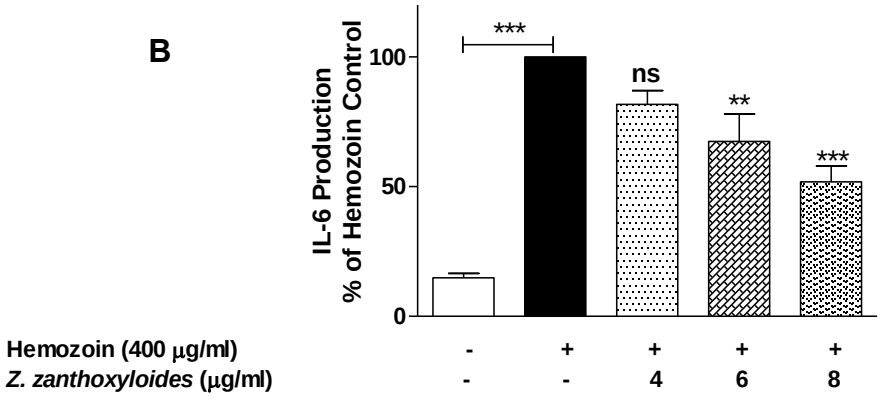
B
IL-6 Production
% of Hemozoin Control
***
ns
**
***
100
50
0
Hemozoin (400 μg/ml)
Z. zanthoxyloides (μg/ml)
- + + + +
- - 4 6 8

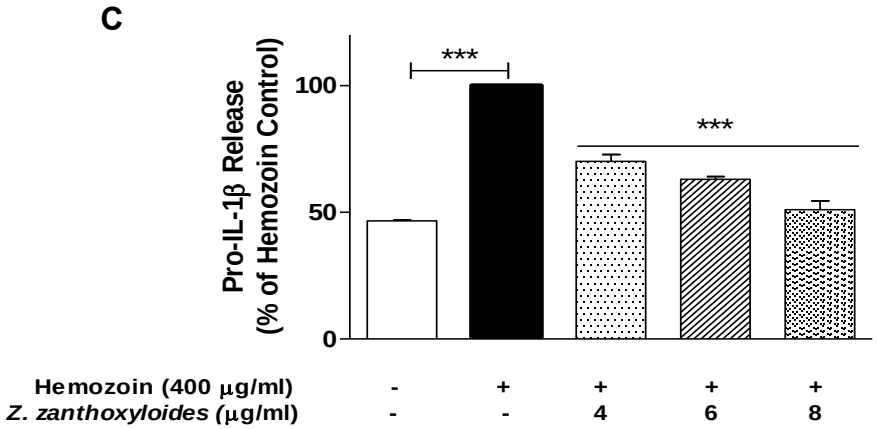
C
Pro-IL-1β Release
(% of Hemozoin Control)
***
***
100
50
0
Hemozoin (400 μg/ml)
Z. zanthoxyloides (μg/ml)
- + + + +
- - 4 6 8

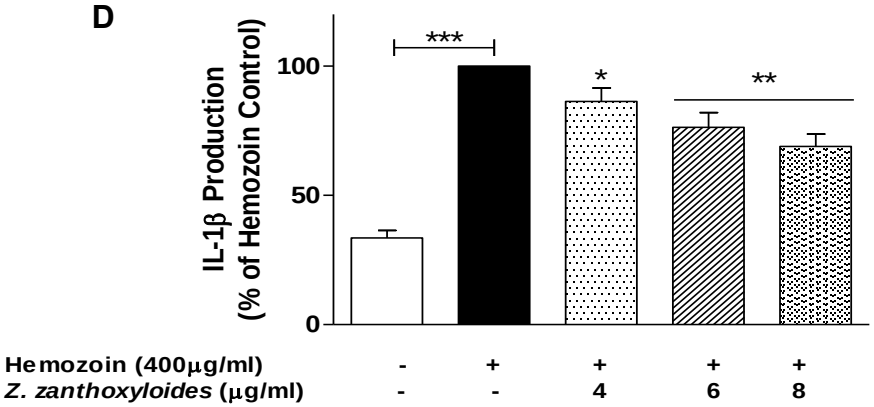
D
IL-1β Production
(% of Hemozoin Control)
***
*
**
100
50
0
Hemozoin (400μg/ml)
Z. zanthoxyloides (μg/ml)
- + + + +
- - 4 6 8

Figure 2

E

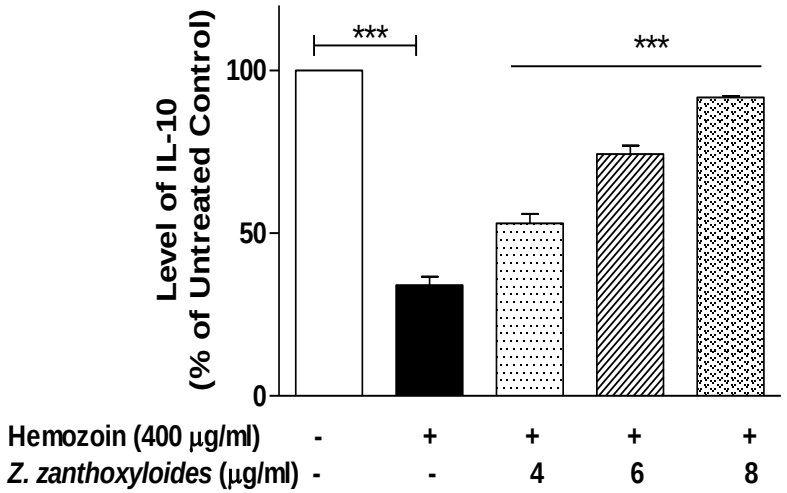
Level of IL-10
(% of Untreated Control)
100
50
0
***
***
Hemozoin (400 μg/ml) - + + + +
Z. zanthoxyloides (μg/ml) - - 4 6 8

Figure 3

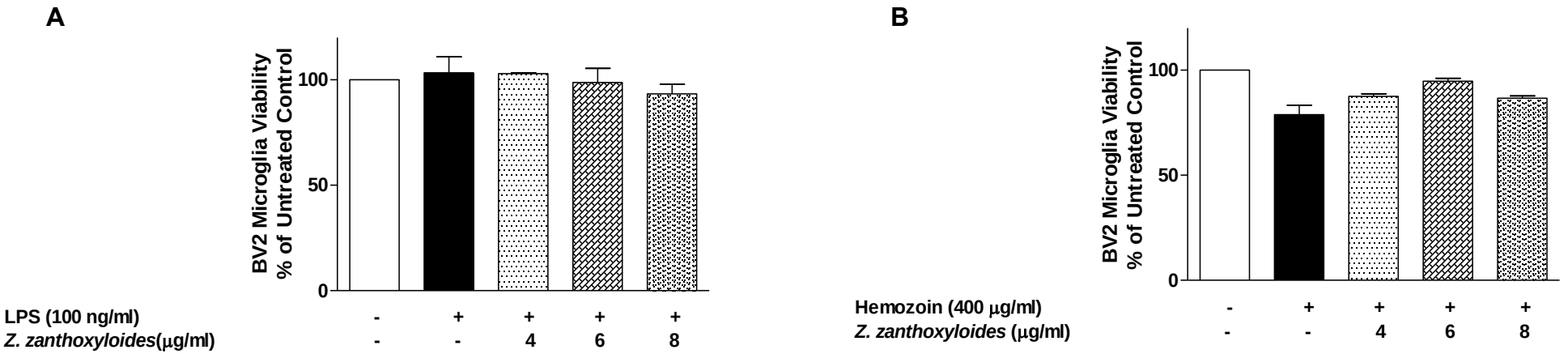
A
BV2 Microglia Viability
% of Untreated Control
100
50
0
LPS (100 ng/ml)
Z. zanthoxyloides(μg/ml)
- + + + +
- - 4 6 8
B
BV2 Microglia Viability
% of Untreated Control
100
50
0
Hemozoin (400 μg/ml)
Z. zanthoxyloides (μg/ml)
- + + + +
- - 4 6 8

Figure 4

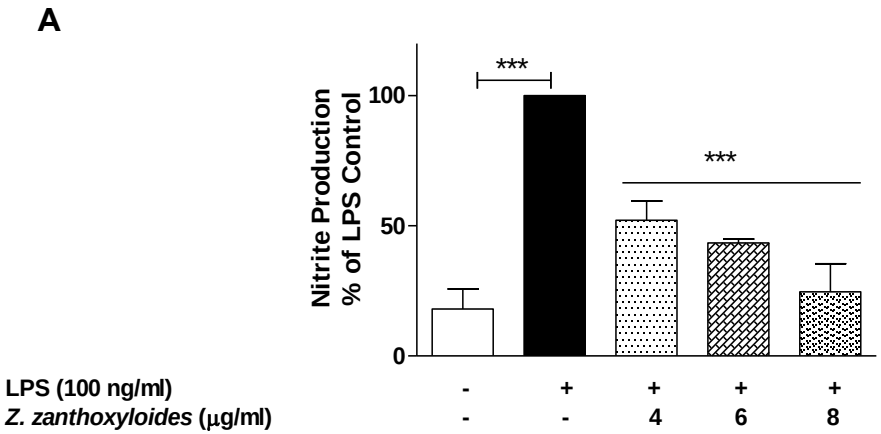
A
Nitrite Production
% of LPS Control
100
50
0
***
***
LPS (100 ng/ml)
Z. zanthoxyloides (μg/ml)
- + + + +
- - 4 6 8

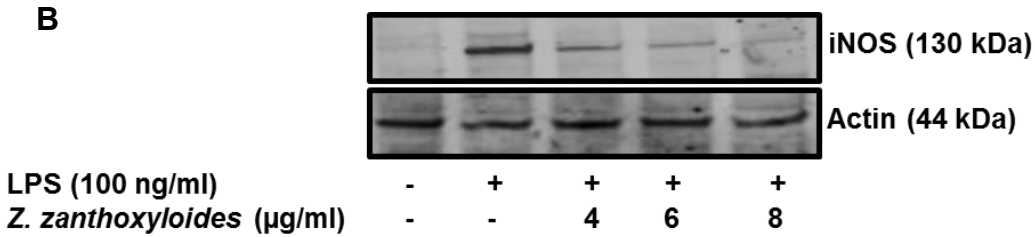
B
iNOS (130 kDa)
Actin (44 kDa)
LPS (100 ng/ml)
Z. zanthoxyloides (μg/ml)
- + + + +
- - 4 6 8

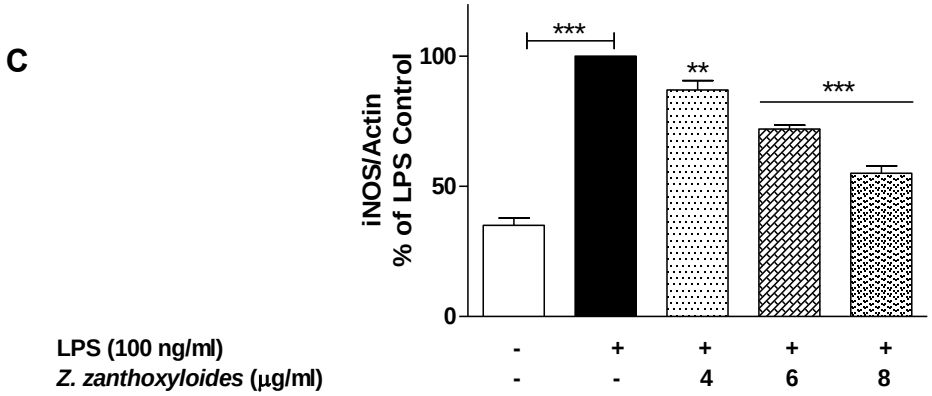
C
iNOS/Actin
% of LPS Control
100
50
0
***
**
***
LPS (100 ng/ml)
Z. zanthoxyloides (μg/ml)
- + + + +
- - 4 6 8

Figure 5

A

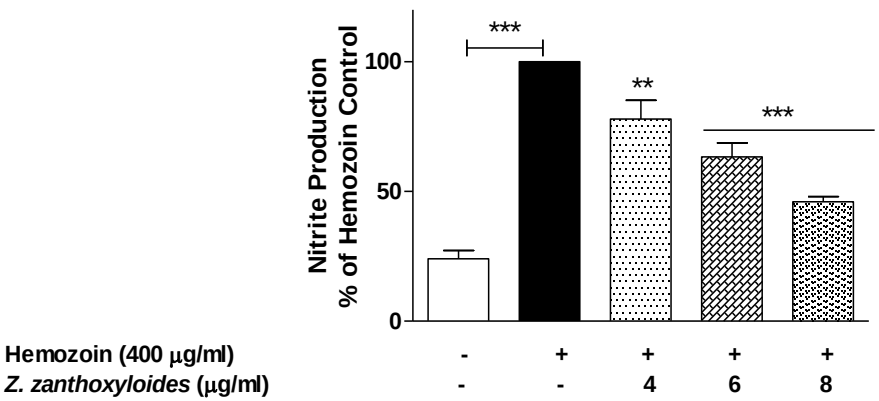
Nitrite Production
% of Hemozoin Control
100
50
0
***
**
***
Hemozoin (400 μg/ml) - + + + +
Z. zanthoxyloides (μg/ml) - - 4 6 8

B

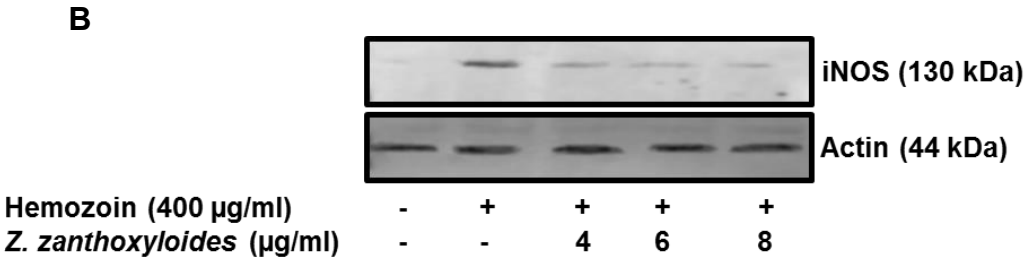
iNOS (130 kDa)
Actin (44 kDa)
Hemozoin (400 μg/ml) - + + + +
Z. zanthoxyloides (μg/ml) - - 4 6 8

C

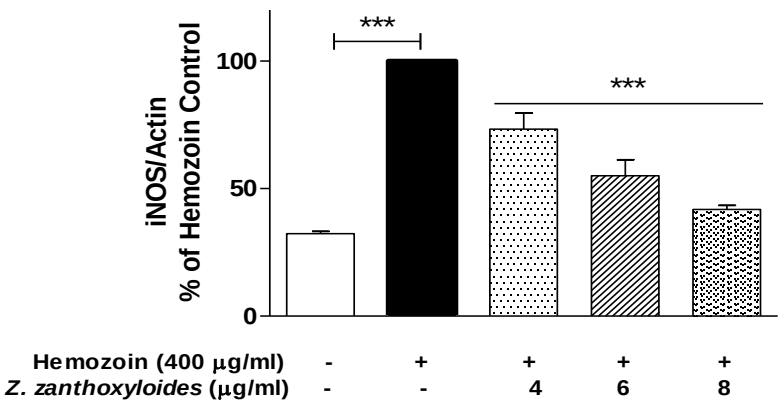
iNOS/Actin
% of Hemozoin Control
100
50
0
***
***
Hemozoin (400 μg/ml) - + + + +
Z. zanthoxyloides (μg/ml) - - 4 6 8

Figure 6

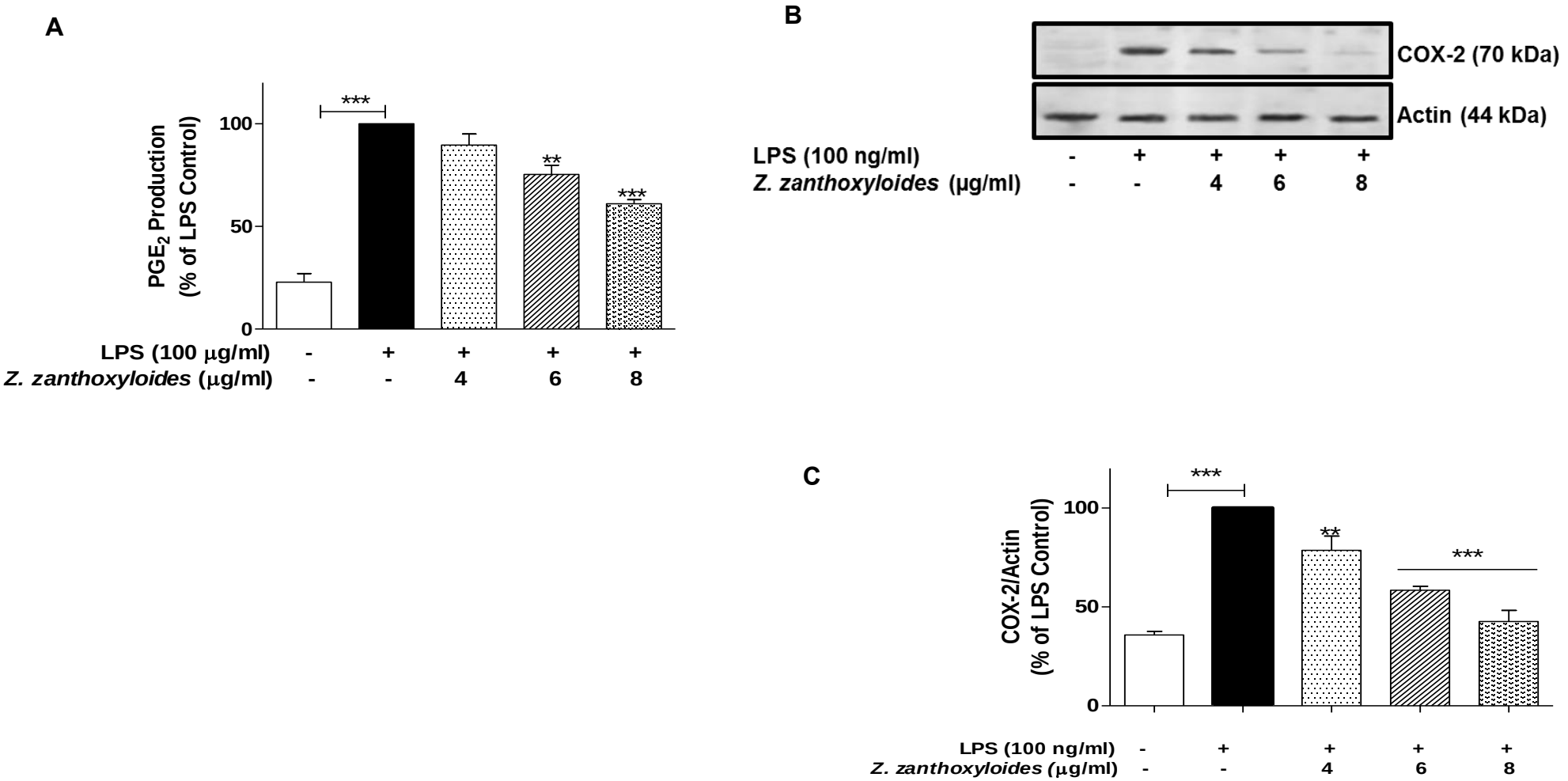
A
PGE2 Production
(% of LPS Control)
100
50
0
***
**
***
LPS (100 μg/ml) - + + + +
Z. zanthoxyloides (μg/ml) - - 4 6 8
B
COX-2 (70 kDa)
Actin (44 kDa)
LPS (100 ng/ml) - + + + +
Z. zanthoxyloides (μg/ml) - - 4 6 8
C
COX-2/Actin
(% of LPS Control)
100
50
0
***
**
***
LPS (100 ng/ml) - + + + +
Z. zanthoxyloides (μg/ml) - - 4 6 8

Figure 7

A

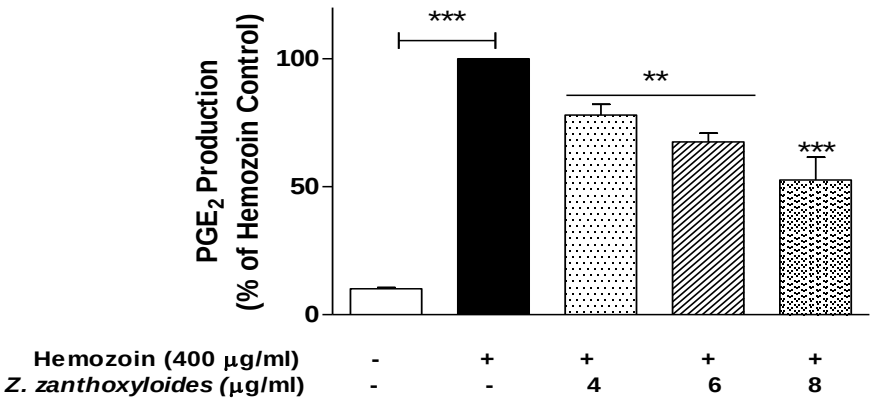
PGE2 Production
(% of Hemozoin Control)
100
50
0
***
**
***
Hemozoin (400 μg/ml) - + + + +
Z. zanthoxyloides (μg/ml) - - 4 6 8

B

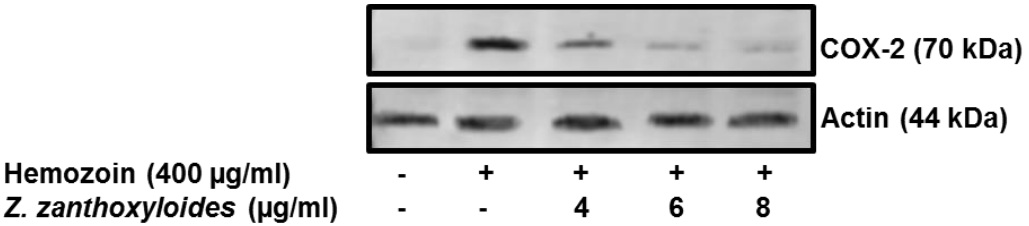
COX-2 (70 kDa)
Actin (44 kDa)
Hemozoin (400 μg/ml) - + + + +
Z. zanthoxyloides (μg/ml) - - 4 6 8

C

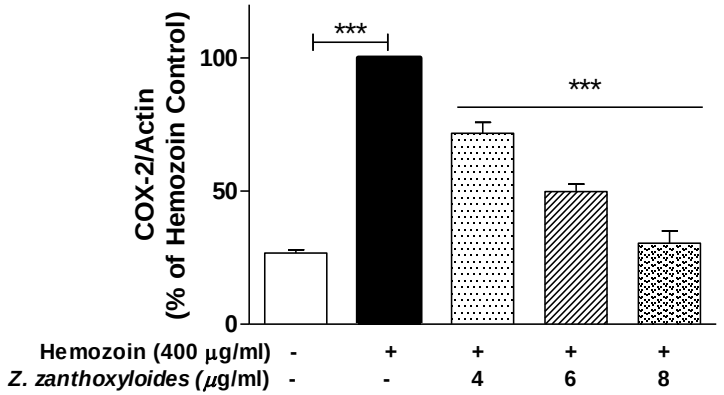
COX-2/Actin
(% of Hemozoin Control)
100
50
0
***
***
Hemozoin (400 μg/ml) - + + + +
Z. zanthoxyloides (μg/ml) - - 4 6 8

Figure 8

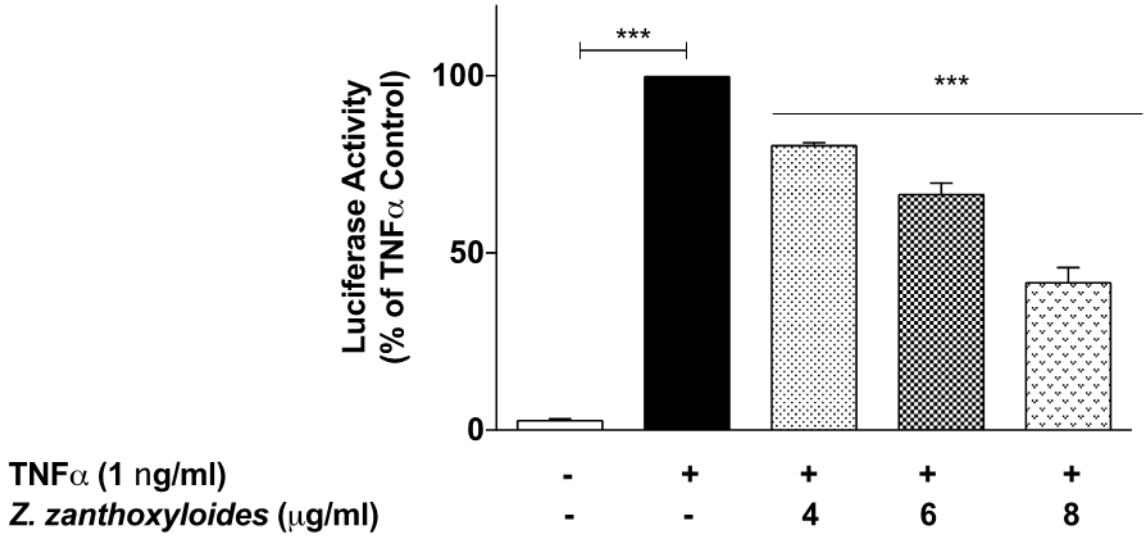
Luciferase Activity
(% of TNFα Control)
100
50
0
***
***
TNFα (1 ng/ml)
Z. zanthoxyloides (μg/ml)
- + + + +
- - 4 6 8

Figure 9

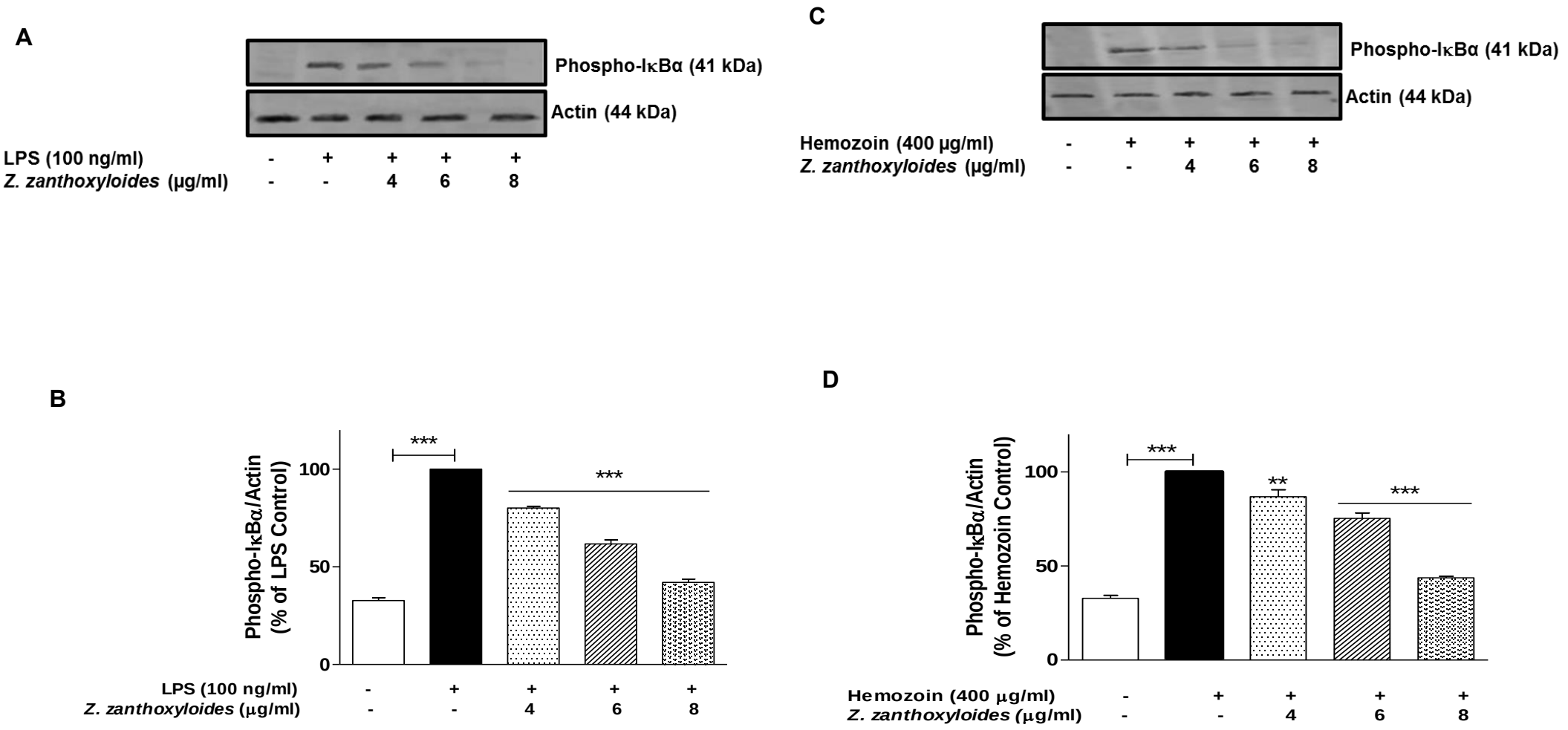
A
Phospho-IκBα (41 kDa)
Actin (44 kDa)
LPS (100 ng/ml) - + + + +
Z. zanthoxyloides (μg/ml) - - 4 6 8
C
Phospho-IκBα (41 kDa)
Actin (44 kDa)
Hemozoin (400 μg/ml) - + + + +
Z. zanthoxyloides (μg/ml) - - 4 6 8
B
Phospho-IκBα/Actin (% of LPS Control)
100
50
0
***
***
LPS (100 ng/ml) - + + + +
Z. zanthoxyloides (μg/ml) - - 4 6 8
D
Phospho-IκBα/Actin (% of Hemozoin Control)
100
50
0
***
**
***
Hemozoin (400 μg/ml) - + + + +
Z. zanthoxyloides (μg/ml) - - 4 6 8

Figure 9

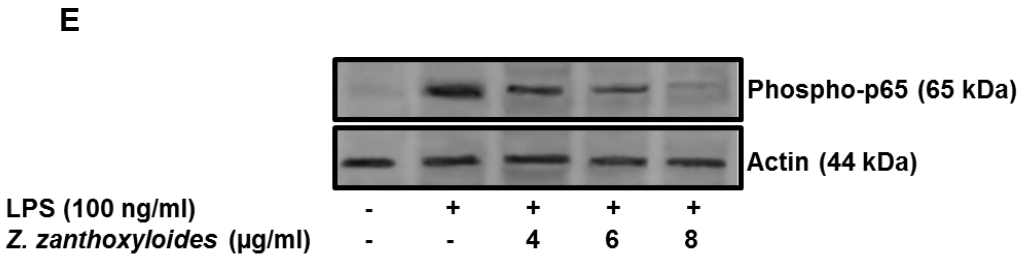
E
Phospho-p65 (65 kDa)
Actin (44 kDa)
LPS (100 ng/ml) - + + + +
Z. zanthoxyloides (µg/ml) - - 4 6 8

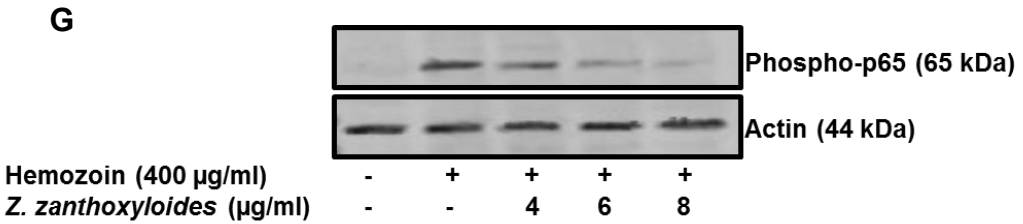
G
Phospho-p65 (65 kDa)
Actin (44 kDa)
Hemozoin (400 µg/ml) - + + + +
Z. zanthoxyloides (µg/ml) - - 4 6 8

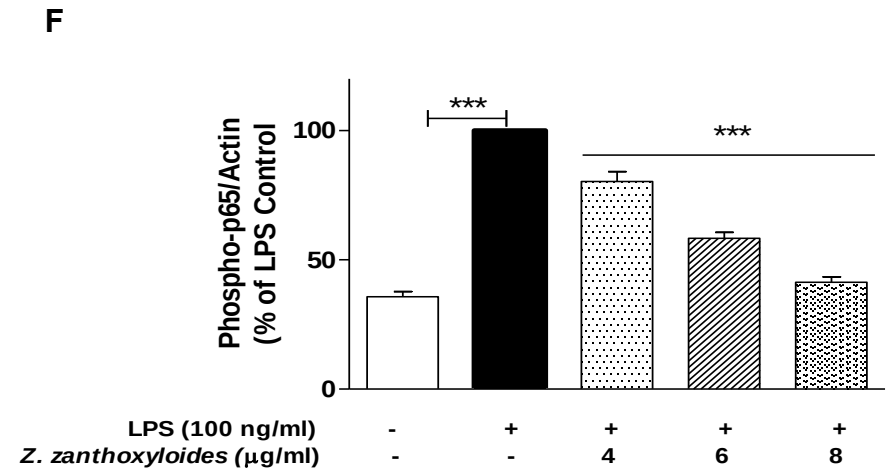
F
Phospho-p65/Actin (% of LPS Control)
100
50
0
***
***
LPS (100 ng/ml) - + + + +
Z. zanthoxyloides (µg/ml) - - 4 6 8

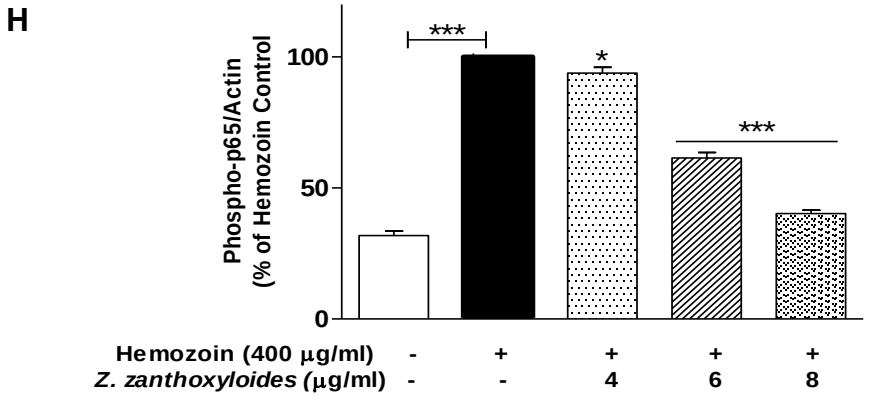
H
Phospho-p65/Actin (% of Hemozoin Control)
100
50
0
***
*
***
Hemozoin (400 µg/ml) - + + + +
Z. zanthoxyloides (µg/ml) - - 4 6 8

Figure 10

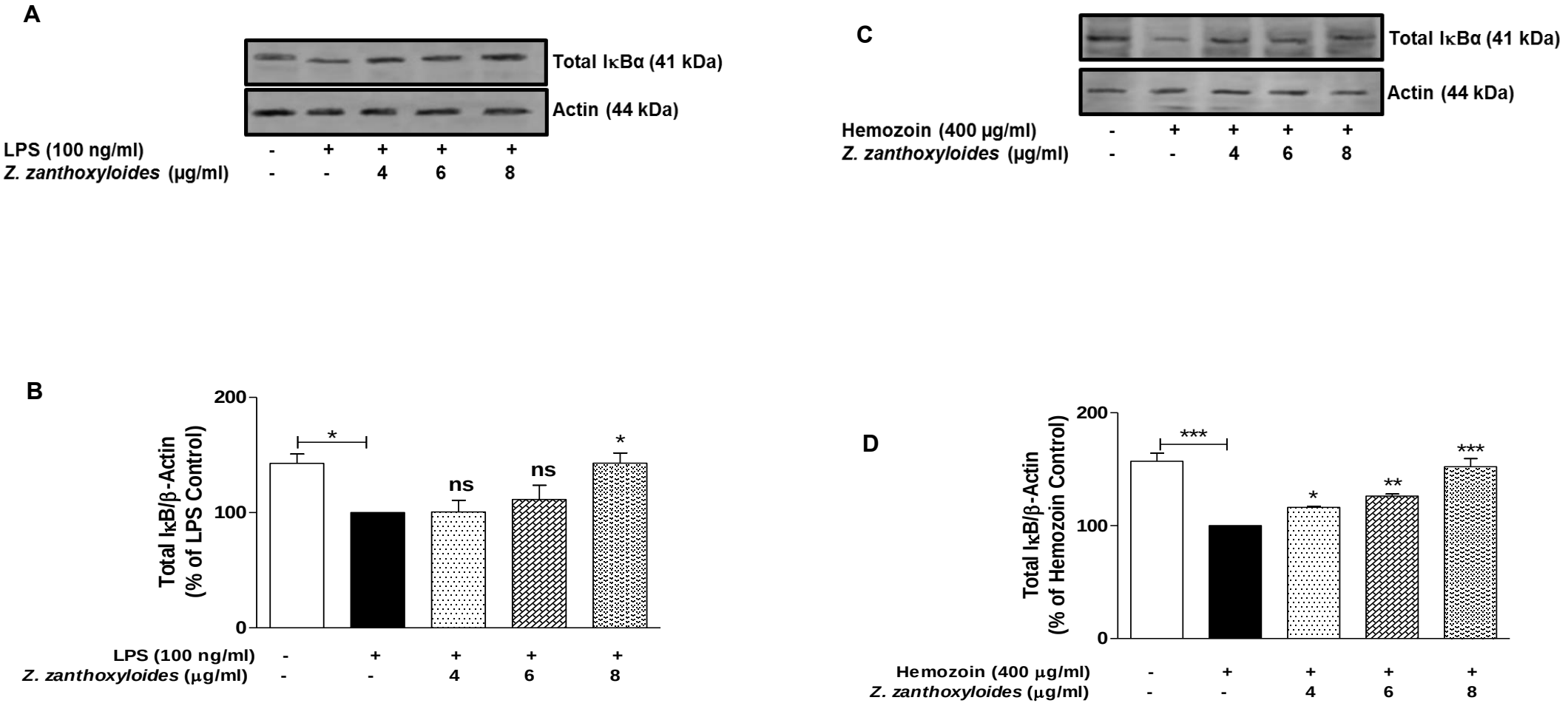
A
Total IκBα (41 kDa)
Actin (44 kDa)
LPS (100 ng/ml) - + + + +
Z. zanthoxyloides (μg/ml) - - 4 6 8
B
Total IκB/β-Actin (% of LPS Control)
200
100
0
*
ns
ns
*
LPS (100 ng/ml) - + + + +
Z. zanthoxyloides (μg/ml) - - 4 6 8
C
Total IκBα (41 kDa)
Actin (44 kDa)
Hemozoin (400 μg/ml) - + + + +
Z. zanthoxyloides (μg/ml) - - 4 6 8
D
Total IκB/β-Actin (% of Hemozoin Control)
200
100
0
***
*
**
***
Hemozoin (400 μg/ml) - + + + +
Z. zanthoxyloides (μg/ml) - - 4 6 8

Figure 11

A

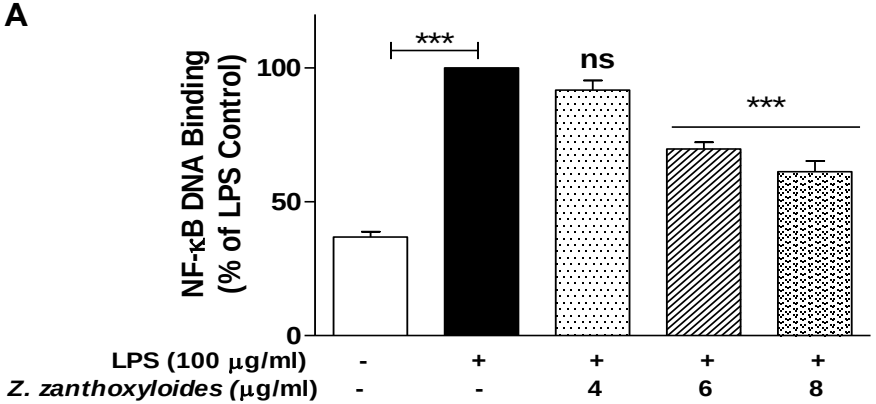
NF-κB DNA Binding
(% of LPS Control)
100
50
0
***
ns
***
LPS (100 μg/ml) - + + + +
Z. zanthoxyloides (μg/ml) - - 4 6 8

B

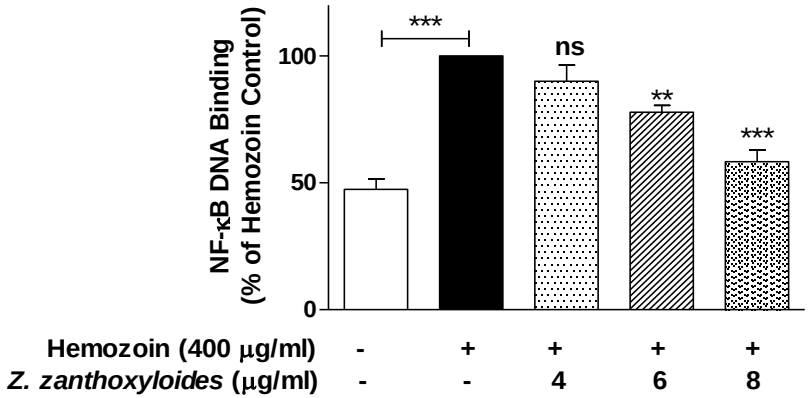
NF-κB DNA Binding
(% of Hemozoin Control)
100
50
0
***
ns
**
***
Hemozoin (400 μg/ml) - + + + +
Z. zanthoxyloides (μg/ml) - - 4 6 8

Figure 12

A

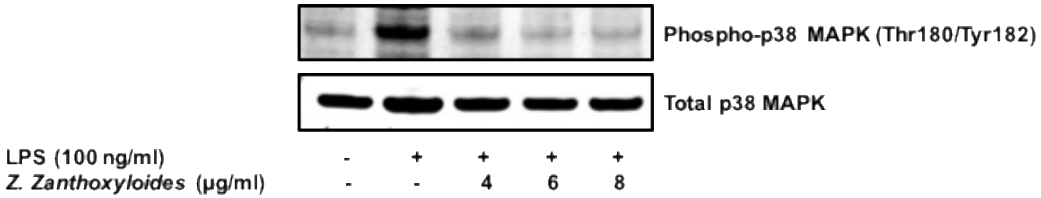
Phospho-p38 MAPK (Thr180/Tyr182)
Total p38 MAPK
LPS (100 ng/ml) - + + + +
Z. Zanthoxyloides (µg/ml) - - 4 6 8

B

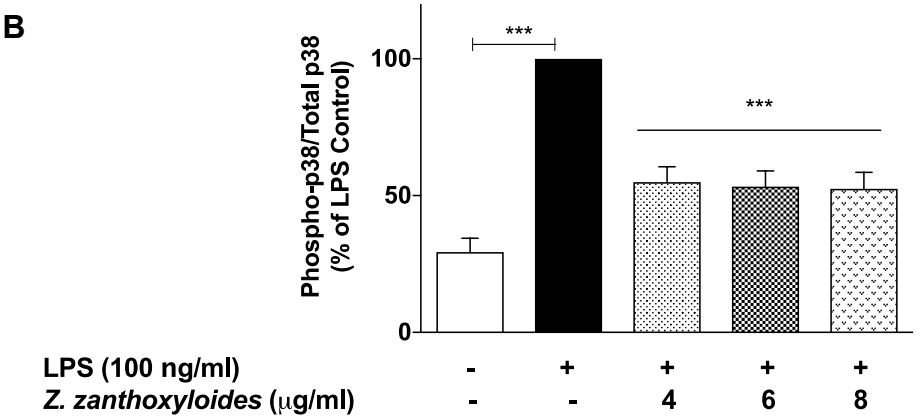
Phospho-p38/Total p38 (% of LPS Control)
100
50
0
***
***
LPS (100 ng/ml) - + + + +
Z. zanthoxyloides (µg/ml) - - 4 6 8

Figure 13

A

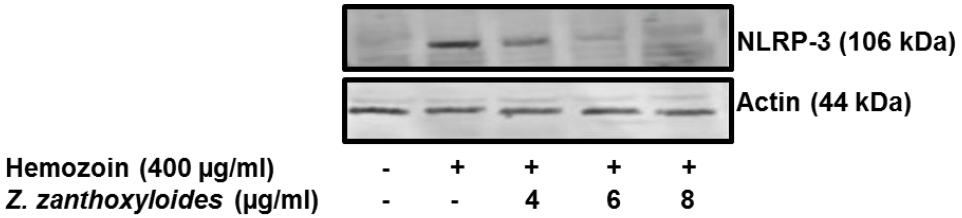
NLRP-3 (106 kDa)
Actin (44 kDa)
Hemozoin (400 µg/ml) - + + + +
Z. zanthoxyloides (µg/ml) - - 4 6 8

B

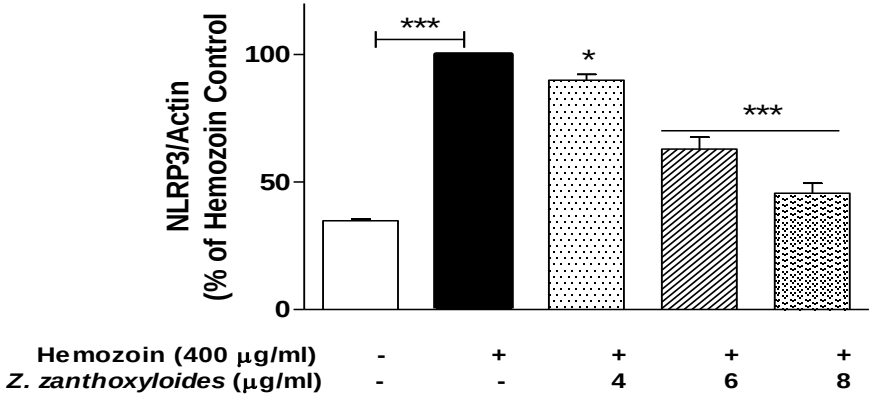
NLRP3/Actin
(% of Hemozoin Control
100
50
0
***
*
***
Hemozoin (400 µg/ml) - + + + +
Z. zanthoxyloides (µg/ml) - - 4 6 8

Figure 14

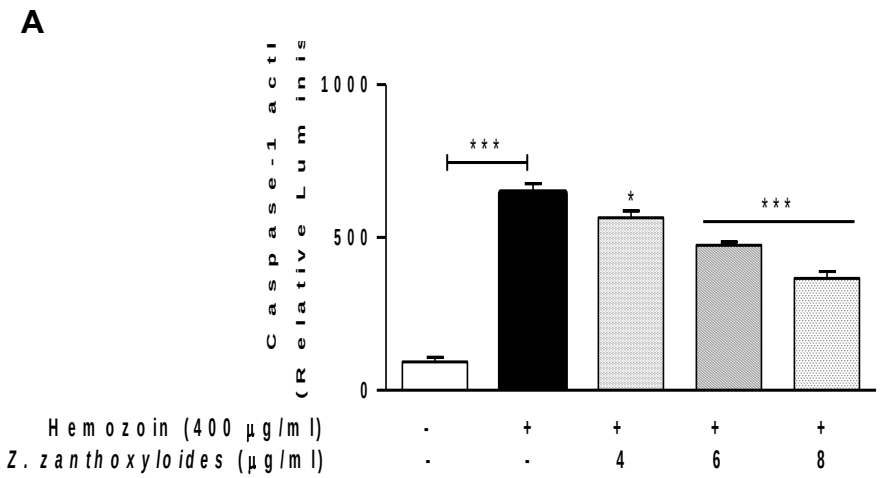
A
Caspase-1 activi
(Relative Lumi inis
1000
500
0
***
*
***
Hemozoin (400 µg/ml) - + + + +
Z. zanthoxyloides (µg/ml) - - 4 6 8

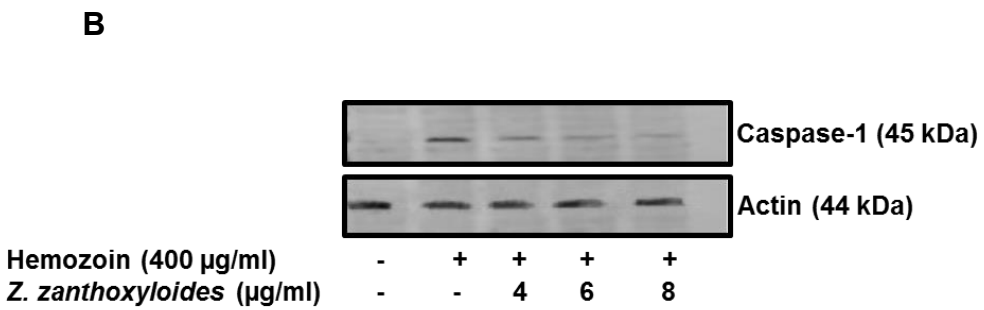
B
Caspase-1 (45 kDa)
Actin (44 kDa)
Hemozoin (400 µg/ml) - + + + +
Z. zanthoxyloides (µg/ml) - - 4 6 8

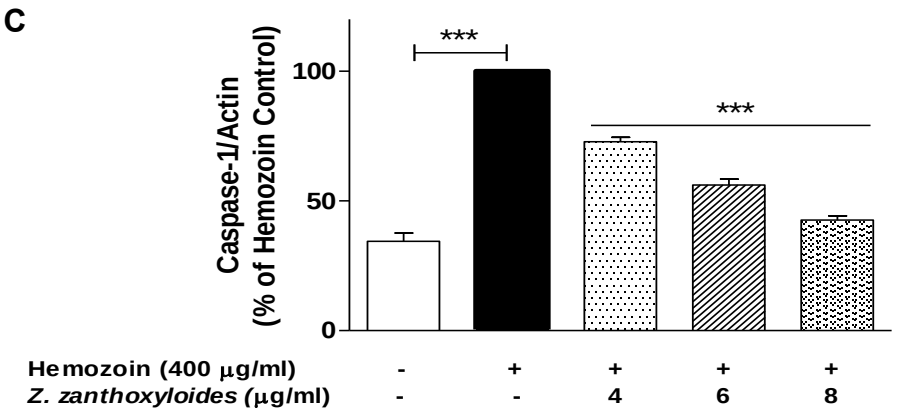
C
Caspase-1/Actin
(% of Hemozoin Control)
100
50
0
***
***
Hemozoin (400 µg/ml) - + + + +
Z. zanthoxyloides (µg/ml) - - 4 6 8

Figure 15

A

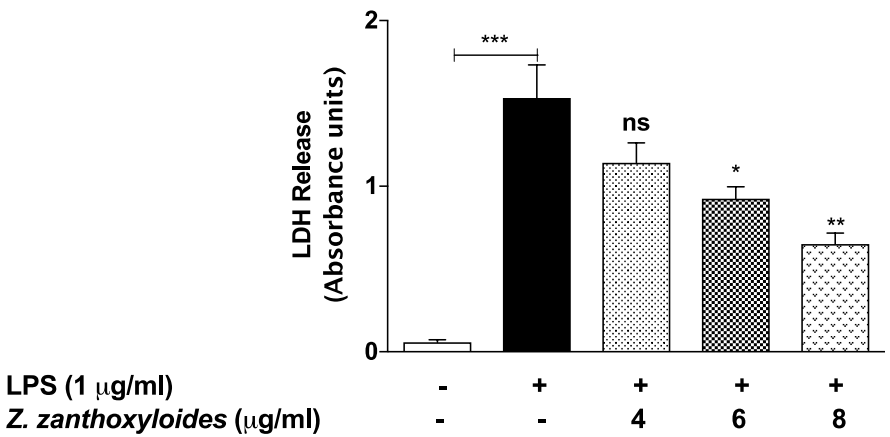
LDH Release
(Absorbance units)
2
1
0
***
ns
*
**
LPS (1 μg/ml) - + + + +
Z. zanthoxyloides (μg/ml) - - 4 6 8

B

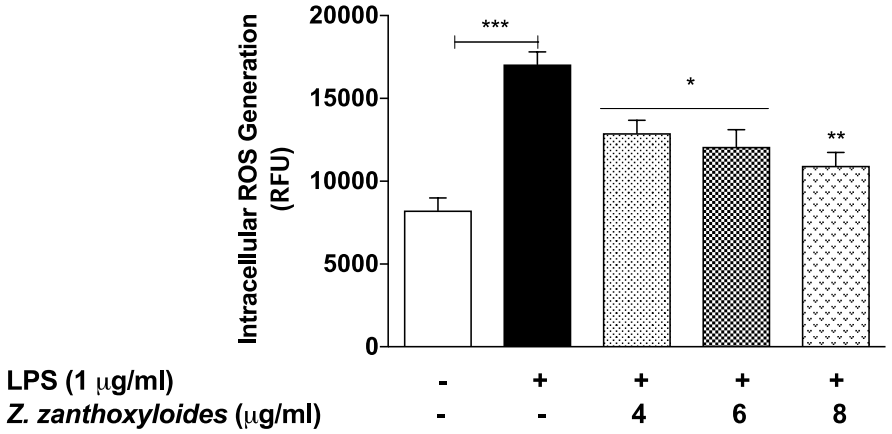
Intracellular ROS Generation
(RFU)
20000
15000
10000
5000
0
***
*
**
LPS (1 μg/ml) - + + + +
Z. zanthoxyloides (μg/ml) - - 4 6 8

Figure 16

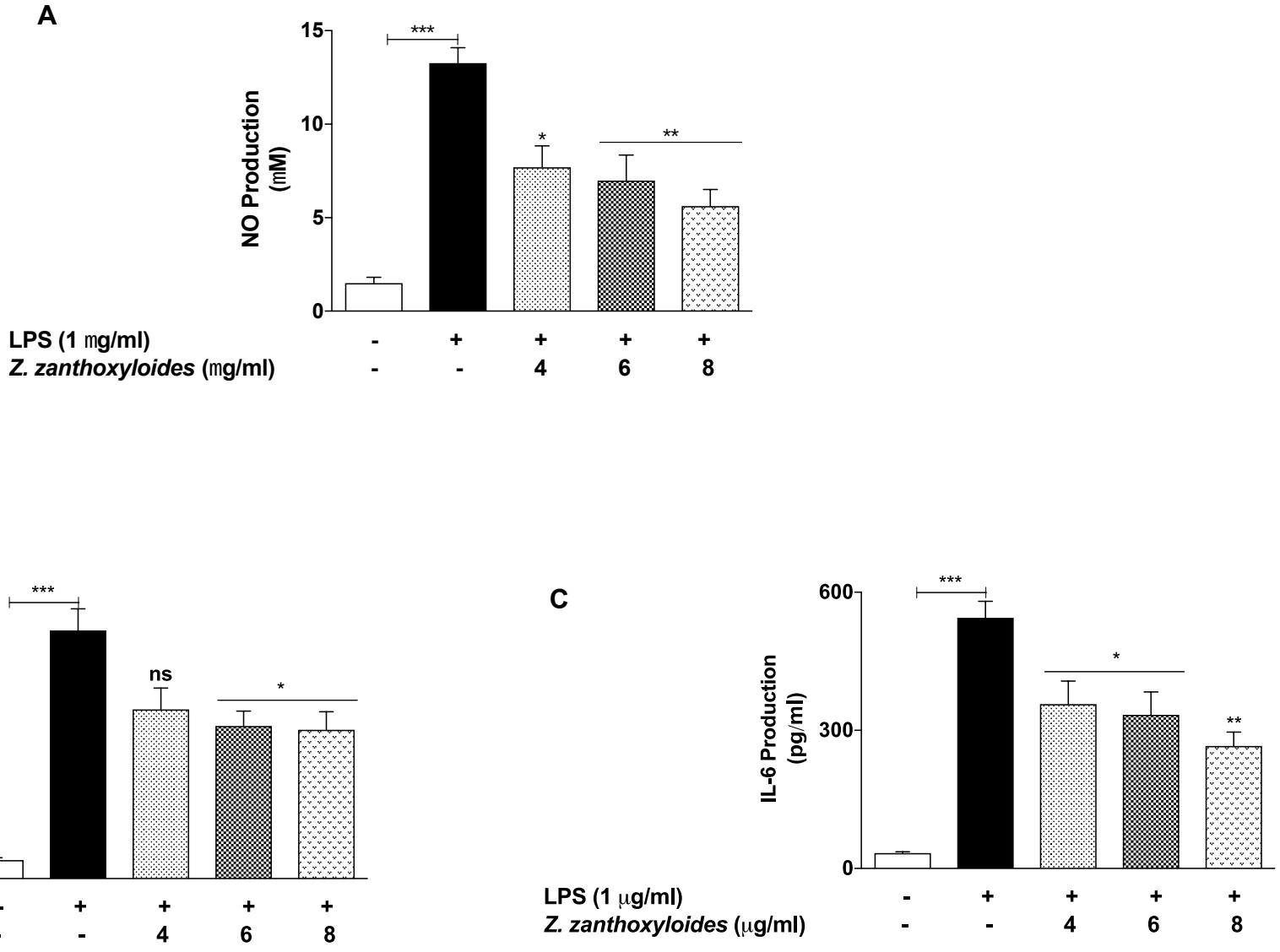
A
NO Production (mM)
15
10
5
0
***
*
**
LPS (1 mg/ml)
Z. zanthoxyloides (mg/ml)
- + + + +
- - 4 6 8
B
TNFα Production (pg/ml)
800
600
400
200
0
***
ns
*
LPS (1 μg/ml)
Z. zanthoxyloides (μg/ml)
- + + + +
- - 4 6 8
C
IL-6 Production (pg/ml)
600
300
0
***
*
**
LPS (1 μg/ml)
Z. zanthoxyloides (μg/ml)
- + + + +
- - 4 6 8

Figure 17

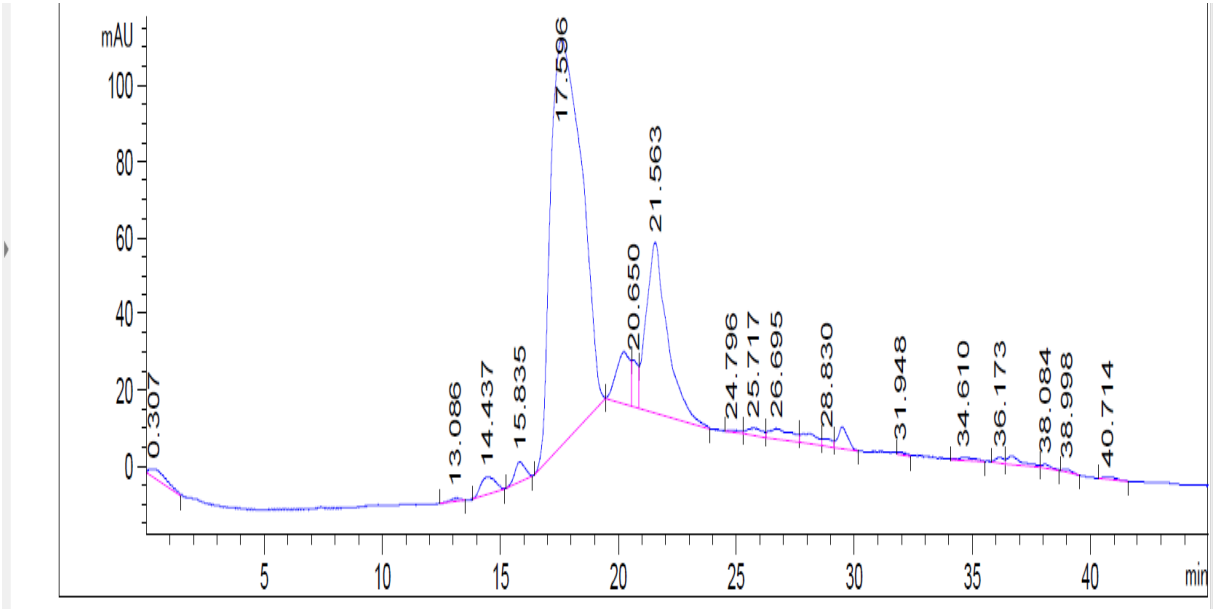
mAU
100
80
60
40
20
0
0.307
13.086
14.437
15.835
17.596
20.650
21.563
24.796
25.717
26.695
28.830
31.948
34.610
36.173
38.084
38.998
40.714
5
10
15
20
25
30
35
40
min

Figure 18

A (Proton NMR of skimmianine)

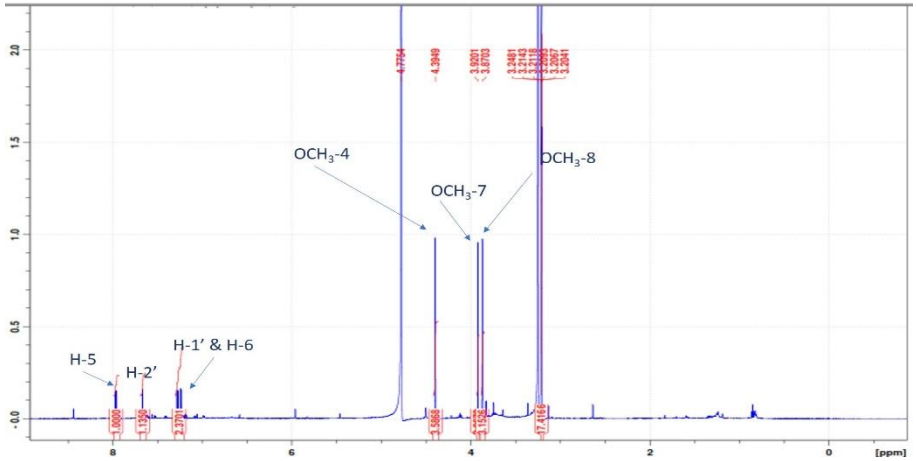

B (Carbon NMR of skimmianine)

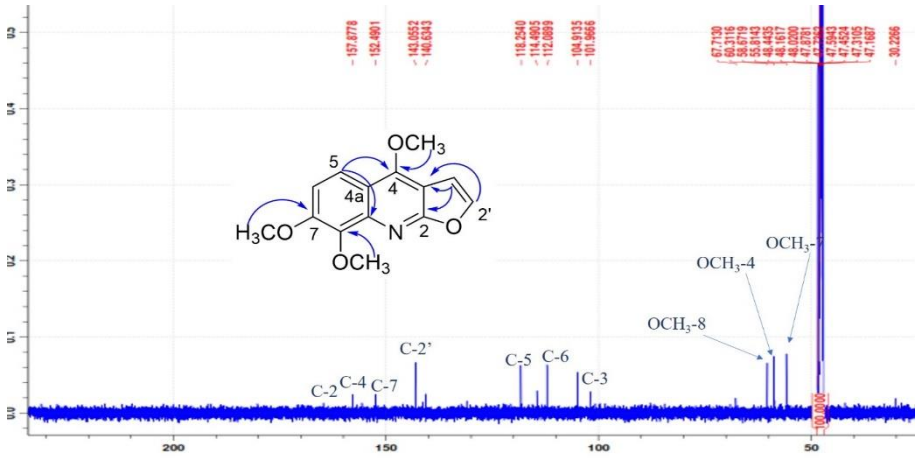

C (1H and Carbon NMR for skimmianine)

Position	δ_C	δ_H *m* (*J* Hz)	HMBC correlation
1	-		
2	164.6		
3	101.9		
4	157.8		
4a	114.6		
5	118.2	8.05 *d* (*9.4*)	4, 7, 8a
6	112.0	7.36 *d* (*9.4*)	6, 7, 8, 4a
7	152.4		
8	104.9		
8a	104.4		
1'	104.9	7.28 *d* (*2.6*)	2, 3, 2'
2'	143.0	7.75 *d* (2.6)	2, 3, 1'
OCH_3-4	58.6	*4.39 s*	4
OCH_3-7	55.8	3.92 s	7
OCH_3-8	60.3	3.87 s	8

D (Mass spectra of skimmianine)

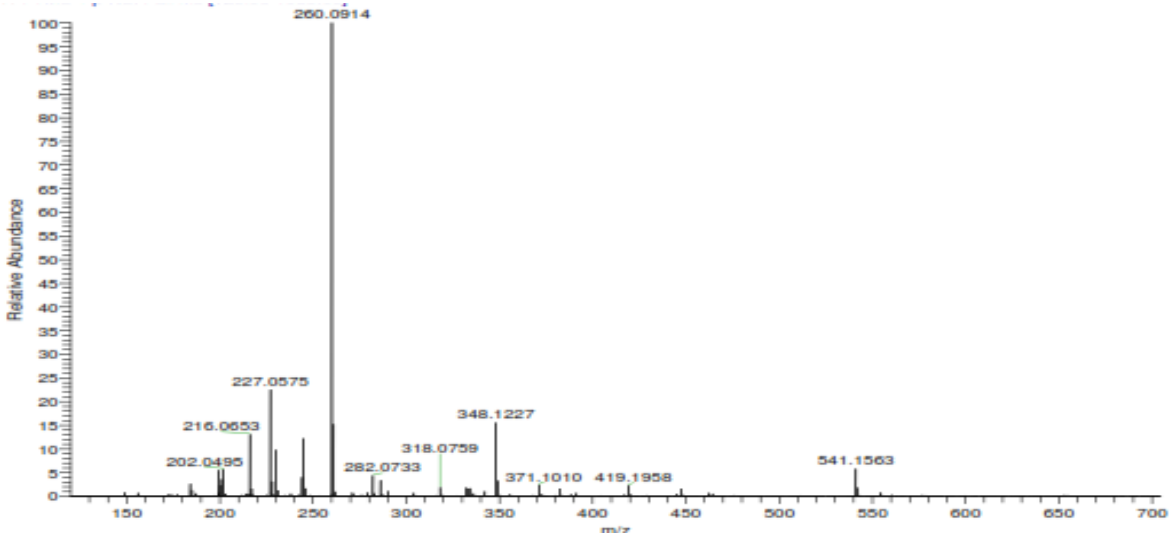

Supplementary Data 1

A

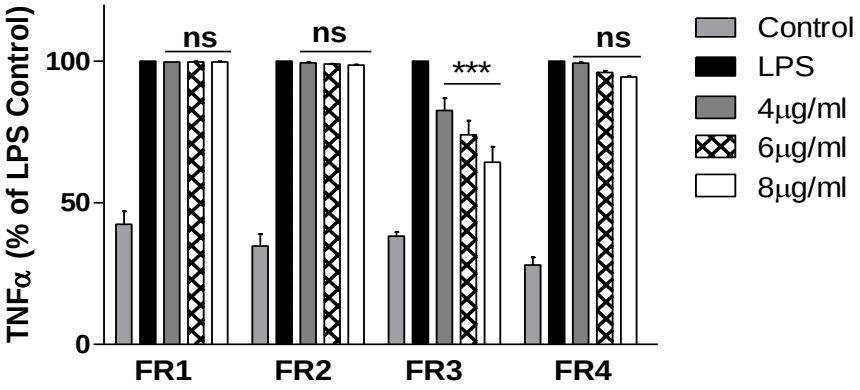

B

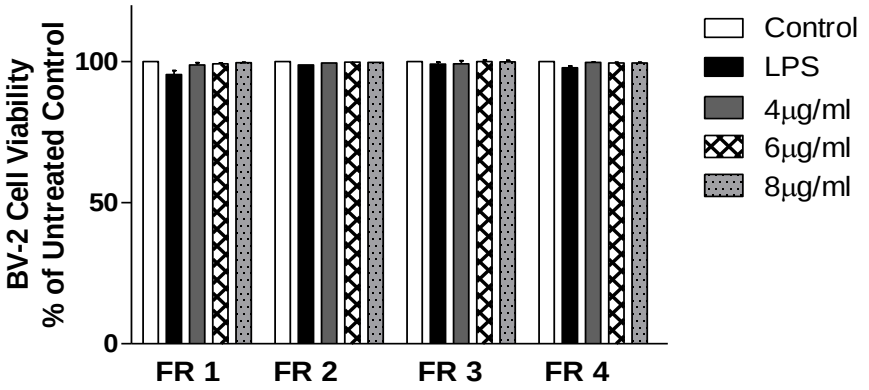

Supplementary Data 2

A

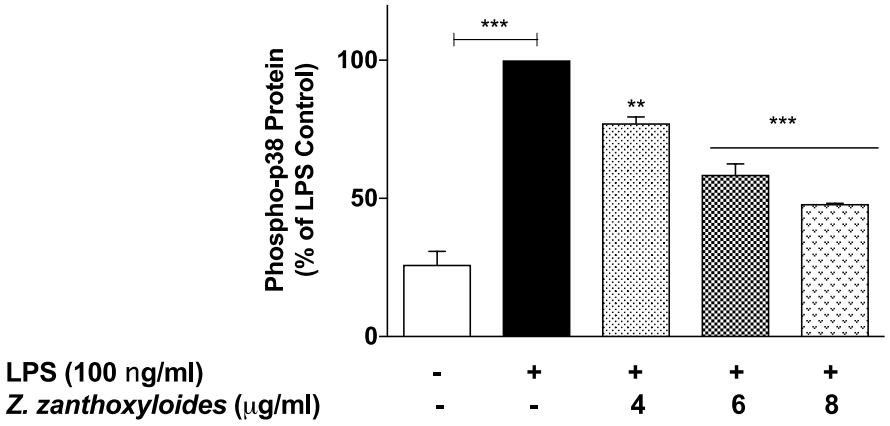

B

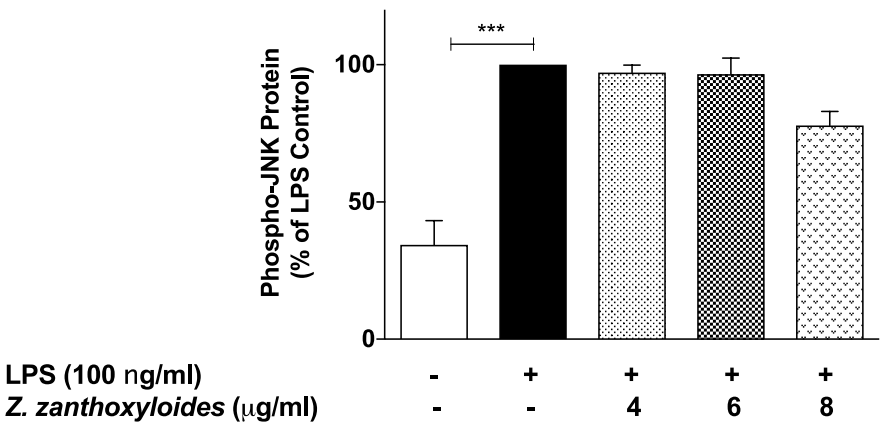

C